PERFORMANCE CHARACTERIZATION OF THE MULTIROTOR UAS CHEMICAL APPLICATION SYSTEM

BY

ADAM P ANDERSON

THESIS

Submitted in partial fulfillment of the requirements
for the degree of Master of Science in Agricultural and Biological Engineering
in the Graduate College of the
University of Illinois at Urbana-Champaign, 2017

Urbana, Illinois

Adviser:

Associate Professor Lei Tian

ABSTRACT

UAS (Unmanned Aerial Systems) have been employed as agro-chemical applicators in agriculture for micro-field applications in Japan, in the form of gas-powered helicopters. A recent surge in battery-powered multirotor UAS has provided a cheaper, more reliable platform that is much simpler to operate. While chemical application systems have been developed for these platforms (mainly in China), fairly little data exists characterizing their performance and identifying ideal operating parameters. The purpose of this project was to attempt to achieve a broad characterization and identify these parameters through collection of spray pattern data produced in a wide array of application conditions. A new test method enclosing the spray system was designed and developed, in an attempt to capture the entire distribution of the spray pattern, and provide information which has not typically been measured. By highlighting important trends that can be applied to similar systems, this information in turn could provide guidelines for the development of future systems in order that they maximize effectiveness through reduction of waste, use of optimal equipment and flight parameters, and minimization of economic loss and ecological damage due to drift and off-target application. The test platform employed was a DJI S1000 octocopter fitted with two TeeJet nozzles ranging from 0.1 to 0.2 gpm flow rate and Fine to Extremely Coarse droplet spectrum range. The findings of this project identified superior coverage density using small droplet spectrum nozzles under the condition that flight height could be maintained at or below recommendations of the nozzle manufacturer (in this case, 0.75 m). Above these heights significant portions of the spray were deposited off-target (up to 50% of droplets) due to downwash outflow, or lost due to meteorological conditions. Droplets in the Medium and Fine spectrum were sensitive to air flow and hence nozzles producing large amounts of these droplets tended to behave less predictably. The more droplets produced under 150 micron, the

more uneven the pattern distribution, as these droplets were disproportionately deposited at the edges of, and outside the target pattern area. Nozzles producing droplets in the Extremely Coarse and Ultra Coarse range were robust to downwash effects and meteorological conditions, displaying an average droplet loss of 17%. This nozzle type also allowed for much more significant deviations in height (ranging from approximately 0.3 to 2 m), at the expense of droplet coverage density, but displaying little variation in effective pattern width. This may suggest this system configuration is better suited for site specific application, where flow rate can be increased, or velocity can be decreased to improve density, and maximizing coverage area is not a primary concern. The enclosed system used in the final tests demonstrated an increase in the percentage of the pattern captured when compared to typical pattern measurement techniques, such as those used in earlier tests, highlighting the advantages of this collection method for complete pattern analysis.

ACKNOWLEDGMENTS

I would like to extend my gratitude to Dr. Lei Tian for his assistance and support in the completion of this project and document. Additionally I would like to thank Dr. Hang Zhu, Matt Gill, Scott Bretthauer, Tim Lecher, Dr. Longzhe Quan, and Dr. Lijuan Yu for their assistance with the initial test procedures and data compilation. Finally to TeeJet and Becky May for the donation of materials essential to the completion of this project, and DJI for the donation of the UAS platform on which the spray system was built.

I would especially like to thank my uncle and aunt, Donald and Loraine Sanchez, whose support made the completion of this work possible.

TABLE OF CONTENTS

LIST OF ABBREVIATIONS

UAS	Unmanned Aerial System
ODAQ	Onboard Data Acquisition System
XR	Extended Range
TT	Turbo Teejet
TTI	Turbo Teejet Induction
GPS	Global Positioning System
VMD	Volume Mean Diameter
LiDAR	Light Detection And Ranging
IMU	Inertial Measurement Unit
LiPo	Lithium Polymer
ULV	Ultra-low Volume
ASABE	American Society of Agricultural and Biological Engineers
USDA	United States Department of Agriculture
CV	Coefficient of Variation
GPA	Gallons per Acre
RAM	Random-Access Memory
SRAM	Static Random-Access Memory
ADC	Analog-to-Digital Converter

CHAPTER 1

BACKGROUND

Current methods of chemical application in agriculture are primarily performed utilizing heavy machinery and aircraft in developed nations. In other parts of the world, or where this type of equipment cannot be utilized (such as hilly regions), application is performed on a smaller scale, through various methods ranging from remote controlled aircraft, small off-road vehicles, or individual application by hand-held sprayers. Increased pressure to improve efficiency while also reducing waste and damage to unintended targets through drift and off-target application, is currently driving the development of more advanced versions of these systems.

While small scale aerial application has been performed for some time in various parts of the world, most systems are based on older platforms like gas powered single-rotor helicopters (Figure 1.1) [1]. A recent surge in multirotor UAS platforms has flooded the market with cheap alternatives to previous small unmanned aircraft. Existing chemical application equipment has successfully been retrofitted to these platforms, and forms of precision application has even been accomplished through use of GPS path planning. Still very little information is available regarding how these systems differ in performance from previous systems, and much of their characteristics are not well understood or optimized. Questions, that if more thoroughly answered, could identify potential applications for these systems that were previously not considered, and increase the efficiency of their utilization, making them a more competitive option for small scale, or even large scale precision application.

Figure 1.1: UAS Applicator

Modern multirotor UAS operate on battery power, primarily LiPo batteries, while some have carrying capacities up to 15L (4 gallons), they are limited by their flight time usually ranging between 15-20 minutes when carrying a payload [2]. Because of the limited payload capacity, much of UAS application is ULV, in order to maximize the amount of chemical that can be applied with the given tank capacity. While Ultra-low Volume does not have a fixed definition, it is generally considered to describe application rates at or below 1 L/ha [3].

1.1 Drift and Off-Target Application

In pesticide application, drift is defined as any part of the application deflected off target by wind [3]. In aerial application the spray system itself can also contribute to drift and off-target application due to air currents created by the propulsion systems. Spray drift can be a significant concern non-target organisms outside the treatment area are sensitive to chemicals being applied. This can include anything from other crops, native vegetation or animals (including humans). Poisoning from pesticides represents a very real

threat in developing countries with poor regulation, regulatory enforcement, inadequate application technology, or without access to education regarding proper application methods. The World Health Organization statistics estimate nearly 200,000 people died globally in 2012 from unintentional pesticide poisoning, and exposure resulted in a cumulative loss of 10.7 millions years of healthy life due to side effects such as disabilities and birth defects [4].

Beyond ethical ramifications, off-target application can be a source of reduced chemical efficacy [5], especially with smaller systems such as UAS where the spray pattern width is very small and high precision is needed to apply the intended amount. This project was also intended to characterize off-target application for this type of system, and infer operating conditions which lead to it.

1.2 Droplet Behavior

A spray pattern can be viewed as a sum of the behavior of the individual droplets formed by spray nozzles. Values used to characterize spray patterns are all influenced by the types of droplets a nozzle produces and the characteristics they possess. Pattern characteristics typically assessed for an applicator include:

- Effective Swath Width - An estimate of the width of the spray pattern that is deposited on a target region.
- CV - Coefficient of Variation is a measure of the continuity of a spray pattern.
- Density - How many droplets are contained in a region (drop/cm^2).
- VMD - Volume Mean Diameter is a method of representing the average droplet size.

These and other values will be discussed in further detail later in Section 2.4.

Droplet behavior, based on characteristics of the droplet and weather conditions, can offer some insight into the analysis of spray pattern distribution. Droplet fall time is determined by the droplet terminal velocity, estimated by Stokes Law (Equation 1.1).

$$V_t = \frac{gd^2Q_d}{18n} \tag{1.1}$$

Where V_t is terminal velocity (m/s), g is gravitational acceleration (m/s^2), d is the initial droplet diameter (m), Q_d is the density of the droplet (kg/m^2), n is the viscosity of air (N·s/m^2). Released from a height of 3 meters, a 50 micron droplet can take 40 seconds to fall, while a 500 micron droplet only 2 seconds.

Expanding on this, a droplet's direction of travel relative to its angle and velocity upon formation, is subject to the following vectors: droplet exit velocity and angle V^X, velocity perpendicular to the ground Vf due gravity, mean wind velocity V^X, and turbulence V^Z which can act in the opposite direction of gravity depending on convection forces. Larger droplets will be more heavily influenced by gravitational forces than any, while small droplets will be heavily influenced by wind and turbulence [7].

Effects of evaporation can also play a significant role in altering droplet characteristics between the time they are produced and impact a surface, based on weather conditions. Droplet lifetime can be estimated through the following Equation 1.2:

$$T = \frac{d^2}{80\Delta T} \tag{1.2}$$

T being the time until extinction (s), d the droplet diameter (m), and ΔT the difference in temperature between wet and dry thermometers (°C) which is a measurement of relative humidity. A 50 micron droplet can experience extinction times as low as 4 to 14 seconds at temperatures ranging from 20-30°C and 50-80% RH, while a droplet of 200 micron could last 65-227 seconds in the same conditions. It should be noted that these values are specific to water, which was the liquid used for these tests. Oil based applications, highly volatile pesticides, or the utilization of other additives can alter these evaporation times.

While this assessment was not intended as an attempt to characterize specific air patterns from the UAS itself, common airflow patterns from rotor aircraft offer a necessary insight into potential influencers of droplet behavior. Rotor blade tips generate downwash as by-product of lift, which manifests itself as an apparent vortex at the blade tips and a column of air forced downward beneath the rotor [6]. Figure 1.2 illustrates this effect and how

the column of air generates an outflow region as the vehicle enters close proximity to the ground. This effect can also be seen in Figure 1.1 illustrating the potential effect on a spray pattern, as droplets will be subject to these forces as well as meteorological factors.

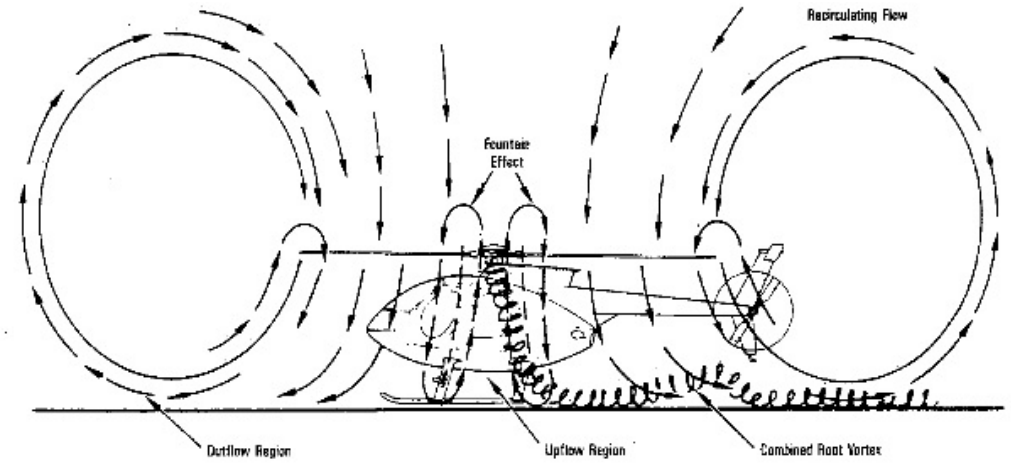

Figure 1.2: Downwash Effects Near the Ground

1.3 Prior Work

Application through UAS has been assessed in areas it is already commonly used, primarily locations that are difficult to employ large aircraft or ground machinery, such as hilly regions or rice paddies. One experiment observe pesticide application in rice paddies using water sensitive paper placed at various levels of the plant, finding an optimum flight height of 1.5m with an application efficacy of up to 92%. This study utilized a quadcopter/fixed-wing hybrid with flight speeds around 5 m/s, and 4 nozzles with flow rates at 0.25 L/min (.07 gpm), resulting in an effective swath width of 4-5 m. These tests however, primarily focused on overall application effectiveness, and not specific characteristics of the pattern and off-target application, with primary metrics being insect control and pattern uniformity [8].

Another study attempted to develop a helicopter platform to improve spray characteristics relative to existing platforms. Test metrics were similar to those used in this study, sampling for droplet characteristics as well as general pattern information. This system attempted to use a roll-balance design in order to reduce downwash bias (uneven droplet distribution due to airflow

patterns from the helicopter rotor). Application heights were as high as 3.5m and measurements were taken using a fluorometer based string system (described in Series 3) as well as water-sensitive paper. Using a 4 nozzle (1 m total width) configuration with a flowrate of 0.4 L/min, the effective swath width was estimated to be 7 m and coverage rates of 20-25% [9].

Determining effects of altering application heights is also important. In one example a study tested deposit on actual crops using a fluorescence spectrophotometer to measure relative deposit on maize plants. A helicopter sprayer was used with 2 centrifugal nozzles at a flow rate of 0.85 L/min (0.2 gpm), and flying at a target velocity of 3 m/s and target heights between 3 and 7 m. This study attempted to vary flight parameters in order to determine how the quality of the spray pattern was effected. It was determined that deposit density at target plants was lowest at 5 m and highest at 7 m. Using CV as a metric of pattern quality, it was observed that CV was a maximum at 5 m and 9 m swath widths (38%) and a minimum at 7 m swath widths (25%) [10].

1.4 Objectives

The previously listed studies provide insight into general behaviors of various types of UAS applicators and their efficacy, primarily focusing on helicopter platforms. Equivalent or more thorough studies for multirotor applicators are currently insufficient to establish the same or better level of characterizing data.

The goal of this project was to use a robust data system to capture a large series of spray pattern information, tracking significant input and environmental variables. Tests were carried out in an outdoor environment, so to account for lack of environmental control only general observations were made regarding performance and influencing factors, while using multivariate statistical analysis methods to identify the most significant influencers of the pattern. By running a wide variety of tests over multiple deposit locations, enough data could be collected to identify important trends while reducing the likelihood of incorrectly attributing results to specific variables. What stands to be gained from this study is determining the unique rates at which spray characteristics decay or improve relative to changes in environmental

conditions and input variables, as well as ideal operating conditions and configurations for multi-rotor applicators. Focusing the important trends and rates at which pattern characteristics change was a defining focus, to ensure the information produced could be applied to a wide variety of systems, and not just the system built in this project.

CHAPTER 2

MATERIALS AND METHODS

This project utilized a custom built spray system and data system, in order to produce the spray patterns and analyze system and environmental conditions during testing. These systems, and the series of tests that were performed to assess the sprayer's characteristics, are described in detail in the following sections.

2.1 Sprayer and Data System

The spray system was built on a DJI S1000 octocopter, which is a UAS designed primarily for professional photography. The platform is intended to carry fairly heavy loads compared to most multirotor UAS (up to 7kg (15lbs)) [11]. The motor size and rotor diameters are suited to balance payload capacity and stability. The spray system built on to the platform was composed of standard sprayer components used for ground systems (hoses and fittings), TeeJet nozzle bodies and nozzles, a small diaphragm pump capable of pressures up to 7 bar (100 psi) and flow rate of 11 L/min (3 gpm), and a flexible liquid bladder to create a sealed environment for the fluid, mitigating the likelihood of air entering the spray system and reducing the shifting of fluid during flight maneuvers. For the purpose of extending the relevance of these results to as many platforms as possible, observations were made primarily on trends concerning pattern and droplet behavior, and less focused on specific values which might vary between platforms.

The data collection system changed between each test series as it was improved and altered. The three main components, which were used in most test series, were a weather station, cameras and an onboard data acquisition system (ODAQ). The general system layout is labeled in Figure 2.1.

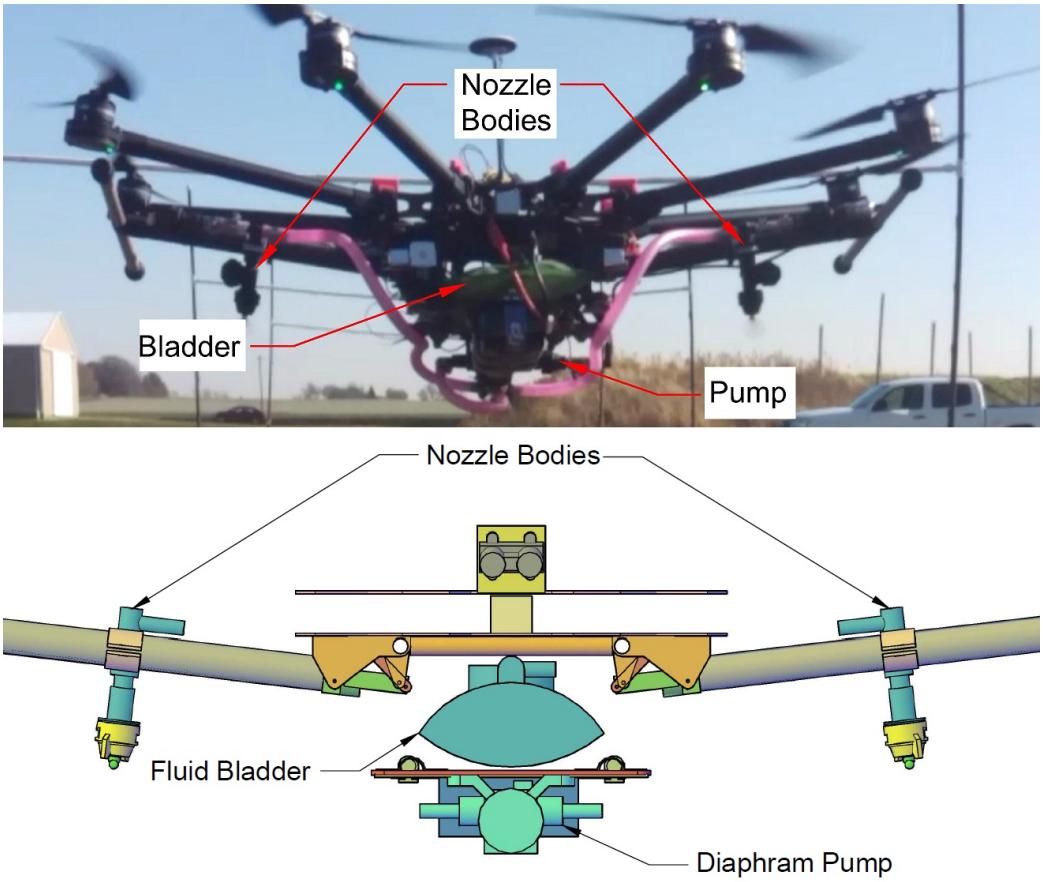

Figure 2.1: Spray System Configuration

All flights in this study were performed under manual control using a Spektrum DX7 transmitter [12]. The DJI S1000 is equipped with fairly robust flight sensors, and additionally can be used with their GPS Ground Station software to plan autonomous flights. However, the altitude estimations are performed through an altimeter based on atmospheric pressure and therefore provided poor accuracy relative to the flight heights used in these tests (approximately 1m). Additionally position estimates were performed through GPS, and the accuracy was also poor (approximately 1.5 m) relative to the width of the flight paths used. Autonomous flight through the built in systems sacrificed the ability to carry out predictable flights and also substantially increased the risk of damaging the UAS.

For Series 1-2 only two of the three systems described above, the weather station and cameras, were used. The cameras used were a smartphone camera and a handheld Samsung video camera. The weather station consisted of a microcontroller and various weather sensors mounted to the frame of a wind-

vane anemometer, with the following specifications highlighting trait relevant to the data collection and design of the system:

1. Microcontroller (Weather Station): Arduino Uno [13]
    - Clock speed: 16 MHz
    - SRAM (Memory for variable storage): 2 KB
2. Temperature and humidity sensor: SHT15 [14]
    - Absolute RH accuracy: 2% RH
    - Temperature accuracy: $\pm$ 0.3 C @ 25 C
3. Barometric pressure sensor: MPL3115A2 [15]
    - Pressure accuracy: $\pm$ 3.6 Pa
4. Wind speed and direction: Wind-vane and cup anemometer [16]
    - Wind-vane resolution: 8 directions
    - Cup anemometer
5. Wireless data communication: XBee 60mW [17]
    - Communication rate: 250kbps Max data rate
    - Communication range: 1 mile (outdoors)

For test Series 1-4, system pressure values were calibrated prior to flight in the lab. The pressure range was set between 1 and 4 bar (approximately 15 and 60 psi) and each increment was calibrated to a corresponding position of an adjustable knob on the transmitter.

The spray system was controlled by an Arduino Uno microcontroller, and pump speed was regulated by a custom built circuit. In test Series 3, the ODAQ was added and flight characteristics were recorded. A single point LiDAR module was connected to the front of the UAS to provide real time distance data. An X-Bee wireless transmitter was connected to the Uno, allowing data to be transmitted and to signal the weather station, so that data could be synced during tests. An SD Card reader was connected to this same shield to allow for onboard data storage. This system is shown mounted to the S1000 in Figure 2.2.

1. Microcontroller (ODAQ): Arduino Uno [13]
    - Clock speed: 16 MHz
    - SRAM (Memory for variable storage): 2 KB
    - ADC Resolution: 10 bit
2. IMU: MPU9150 [18]
    - Tri-axis gyroscope sensitivity: 131 LSBs/dps
    - Tri-axis accelerometer range: ± 2g-16g
    - Tri-axis compass range: ± 1200T
    - Communication rate: 400kHz
3. Wireless data communication: XBee 60mW [17]
    - Communication rate: 250kbps Max data rate
    - Communication range: 1 mile (outdoors)
4. LiDAR: LiDAR Lite [19]
    - Accuracy: ± 2.5 cm
    - Range: 0-40 m
    - Acquisition time: 0.02 sec
5. Data storage: Arduino Wireless SD Shield (microSD card) [20]

Additionally, for Series 3-5 only smartphone cameras were used due to reliability issues with the camera used in Series 2.

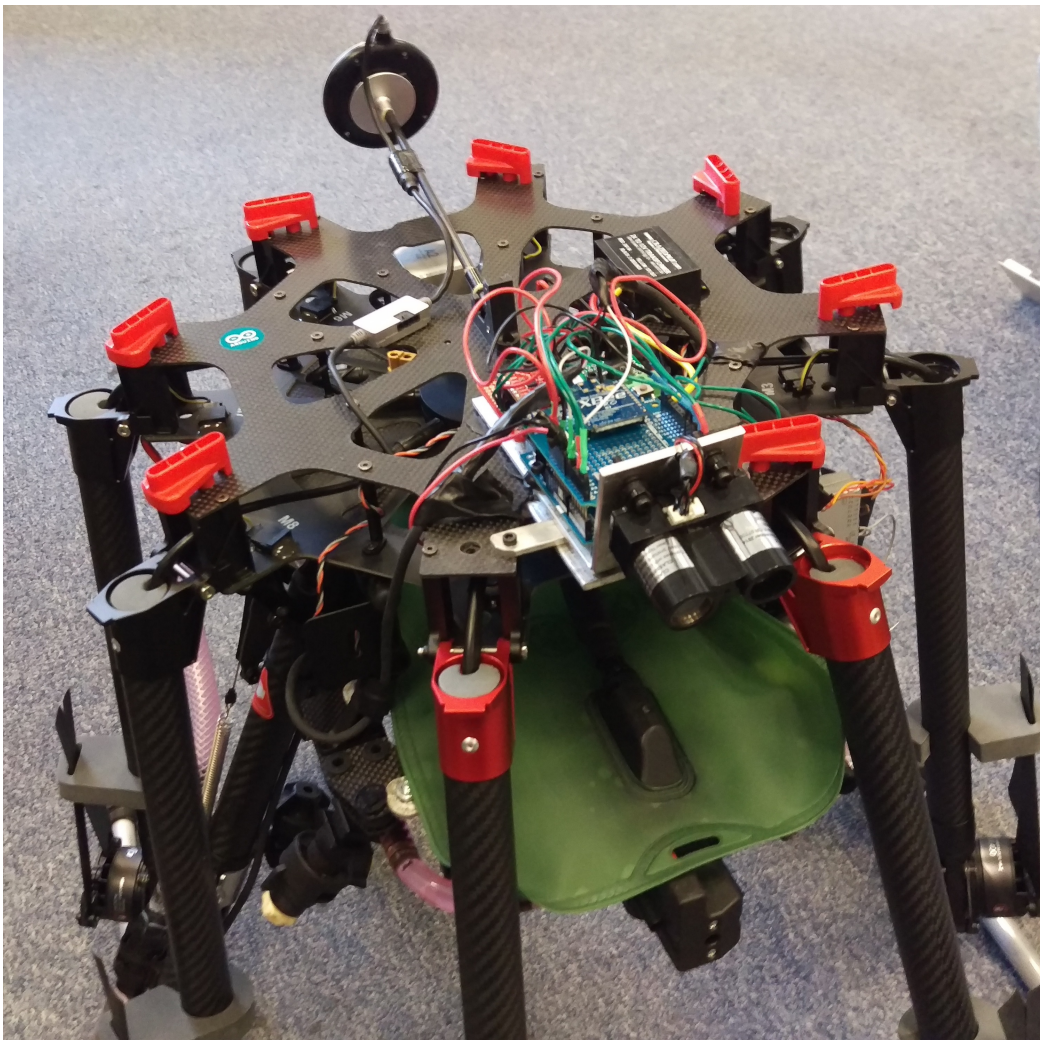

Figure 2.2: ODAQ Design - Iteration 1

For Series 6, the data system was upgraded with a more robust microcontroller (Figure 2.3). The increased analog resolution allowed the integration of an accurate pressure monitor, the high clock speed ensured data acquisition from the sensors was not limited by the microcontroller itself, while the significant increase in SRAM allowed for a more robust data collection program to be stored.

1. Microcontroller: Arduino Zero [21]
    - Clock speed: 48 MHz
    - SRAM (Memory for variable storage): 32 KB
    - ADC Resolution: 12 bit

2. Pressure Transducer: American Sensor Technologies AST4100 [22]

   - Maximum Pressure: 100 psi
   - Output: 10mV/V

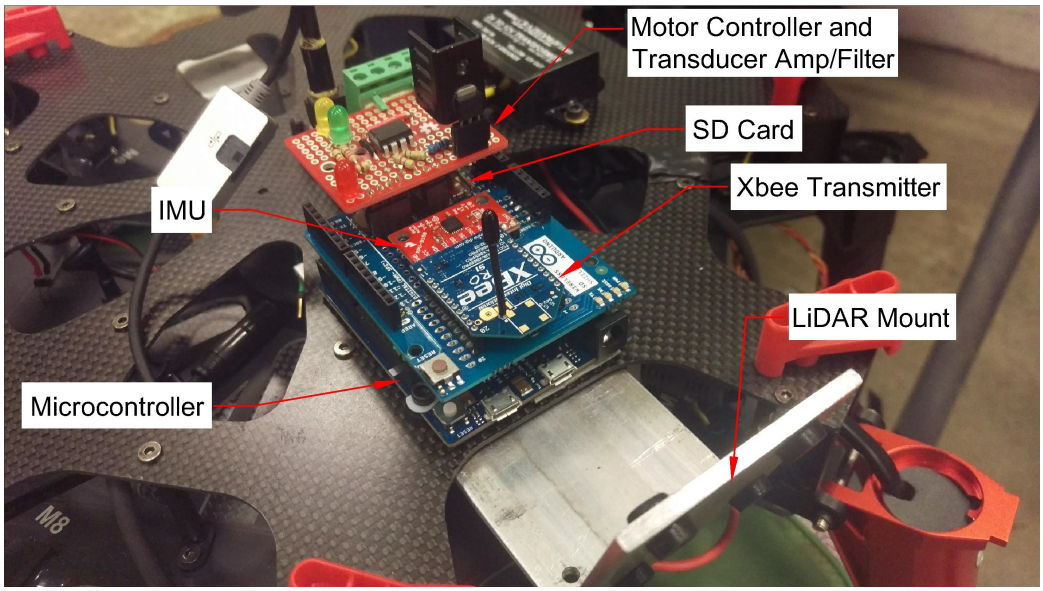

Figure 2.3: ODAQ Design - Iteration 2

Two cameras were constructed for Series 6 to replace the original method of using smartphone cameras (Figure 2.4). The purpose being to standardize the video and establish a more reliable recording method. Additionally the cameras were designed to trigger with the data system, so that the timing would inherently be synced with the ODAQ and weather station data.

The test cameras were built on a Raspberry Pi 3 single-board computer. The computer was fitted with a custom built battery pack and videos were offloaded to an external drive after recording. A simple Python script was written to allow the cameras to be controlled via trigger signals from the weather station and send calibration (alignment since no viewfinder was used) images to a laptop via Bluetooth. Upon receiving the trigger from the weather station, the camera would record a 30 second video clip and transfer it to the external drive.

1. Platform: Raspberry Pi 3
2. Camera (Sensor): Pi Cam [23]

- Resolution: 8MP
- Frame Rate (used): 30 fps

Figure 2.4: Data System Cameras

2.2 Droplet Detection Program

For Series 2-5, droplet analysis was performed using the DepositScan [24] program, made available by the USDA. The program is designed to use a scanner with a resolution of 600 dpi. This meant that the threshold for droplet sizes that would be detected was around 50 micron and the threshold for droplets that could accurately be sized was closer to 100 micron. Other resolutions could be used, but the program would assess them as though they were 600 dpi, so all output data would have to be converted to account for this.

A droplet analysis program was developed in Matlab, with the intention of adapting it for use on a smartphone, this way a higher resolution image could be used and images could be captured in the field before analysis. For this set of tests it was decided that the benefits of capturing images in the field did not outweigh the potential loss in accuracy (due to variability of image quality using a phone camera in the field). Instead the program was

modified to use images from a scanner, but processes such as image cropping and scaling were automated. Higher resolution images could be used than DepositScan was designed for, and the program would adjust the pixel scaling based on the measured card size. Additionally an output was provided for each card in order to allow feedback from the operator to verify results and make changes to thresholds and cropping as necessary. Following the same basic principles used in DepositScan for limiting the size of droplets registered based on resolution, the minimum detectable droplet size was approximately 25 micron when utilizing a 2400 dpi scanner. The general algorithm is listed in the appendix.

2.3 Spray Test Structures

All tests were performed in an outdoor environment. The intention was to partially simulate realistic application conditions, and therefore also adhere to typical guidelines for application environmental conditions. Testing was avoided when wind velocities exceeded 5 m/s (11 mph), attempting to carry out most tests under 3 m/s (7 mph) since most of the nozzles being used produced a smaller droplet spectrum. General application recommendations impose a maximum wind velocity of 3 m/s (7 mph) before increasing droplet size, as well as temperatures under 25°C (77°F) to reduce evaporation and drift potential [25]. Spray tests were structured so that each major test (in which the structure and test method is altered) is referred to as a Series, alterations in the flight parameters (such as a change in nozzle pressure) are separated by Tests, each flight is a Pass, and each data collection station is a Station. These words will be capitalized as such when being referred to in the context of this test structure.

2.3.1 Series 2

Test Series 1 and 2 were preliminary tests performed in order to obtain initial results to decide on the direction of future tests. No data were collected for Series 1 other than video data. Series 2 was the first test series intended to assess information about the details of the spray pattern. For Series 2 a flight line was established, the UAS would be equipped with two different

nozzles and flown along this flight line while spraying, varying the pressure for each flight pass. Along this flight line, 3 frames (2.4 m (8 ft) 2x4 studs with brackets on either end, allowing them to be staked into the ground and leveled) were arrayed perpendicular to the flight line and spaced evenly over a length of 30.5 m (100 ft) between the start and end of the flight (Figure 2.5).

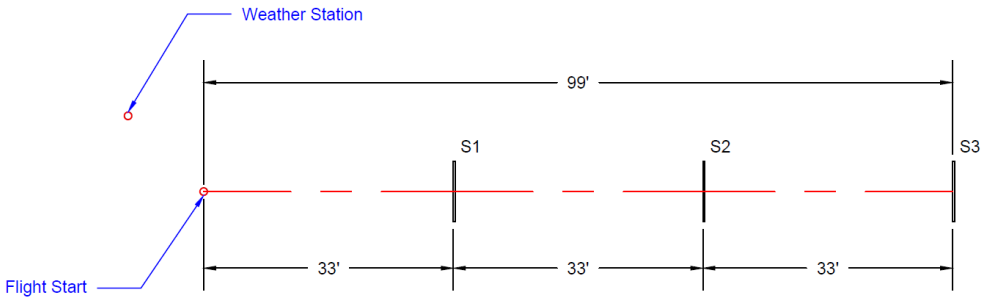

Figure 2.5: Series 2 - Test Layout

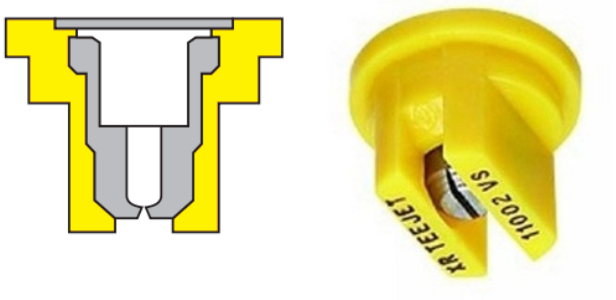

Figure 2.6: TeeJet XR Nozzle

The XR (Extended Range) nozzle was used for most of the initial testing. This is a flat fan nozzle, meaning it produces an even spray pattern in the shape of a flat fan perpendicular to the direction of travel. Extended Range denotes the increased ability to control droplet size and density through adjustments in pressure relative to other nozzles of similar design, with droplets decreasing in size and increasing in quantity as pressure is increased. This nozzle has a single orifice at which fluid flow is controlled and the droplets are produced. Droplet size is classified by the nozzle VMD and falls within a range described by the table shown in Figure 2.7, the XR nozzles used in these tests produce droplets in the Fine range [25].

TeeJet TECHNOLOGIES

Droplet Size Categories

ASABE Standard S-572.1*

Category	Symbol	Color Code	Dv0.5 (VMD)
Extremely Fine	XF	Purple	≈50
Very Fine	VF	Red	<136
Fine	F	Orange	136-177
Medium	M	Yellow	177-218
Coarse	C	Blue	218-349
Very Coarse	VC	Green	349-428
Extremely Coarse	XC	White	428-622
Ultra Coarse	UC	Black	>622

Data Extracted from American Society of Agricultural and Biological Engineers (ASABE) Standard S-572.1. Revised March 2010. Classifications are subject to change.

Figure 2.7: Droplet Size Classification

Each nozzle contains a model number which describes the nozzle (Figure 2.8). The nozzle type is listed first, then the spray angle, followed by the flow rate at 2.8 bar pressure (40 psi). Most existing multirotor sprayers have an upper limit on their carrying capacity of about 1-4 gallons with flight times between 10-20 minutes under a full load [2]. Two flow rates were selected based on depleting a 2 gallon tank in the window of these flight times, all nozzles used in this study were 01 or 02 nozzles (0.1-0.2 GPM).

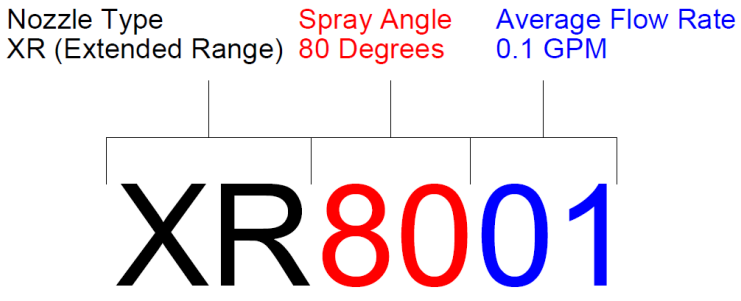

Figure 2.8: TeeJet Nozzle Classification

For all test series excluding Series 3, water-sensitive paper was the primary form of collecting spray pattern data. Water-sensitive paper is a rigid paper

with a specially coated, yellow surface, which is stained dark blue by aqueous droplets impinging on it [26]. A sample of a card which has been exposed to spray droplets, can be seen in Figure 2.9. Water sensitive paper provides a snapshot of a section of the spray pattern containing information about droplet density and size. Placed in an array, these cards can provide insight into details of the full spray pattern of an applicator. The stations described in this test contained an array of water sensitive paper spaced according to Figure 2.10. The spacing decided on for this test Series was 0.3 m (1 ft). Estimated pattern width for a pair of 80° nozzles with a spacing of 0.5 m (20 in) at the suggested flight height of 0.76 m (30 in) is approximately 1.5 m (5 ft) [25]. A total measurement width of approximately 1.8 m (6 ft) was used.

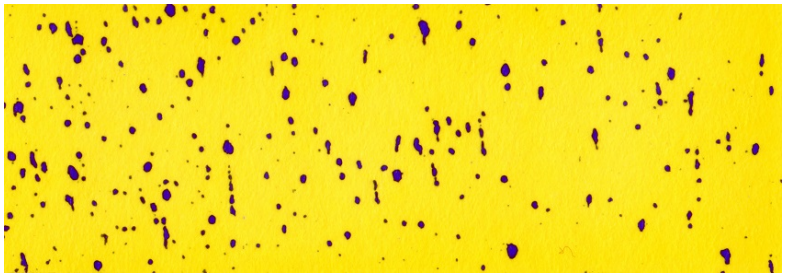

Figure 2.9: Sample Droplet Card

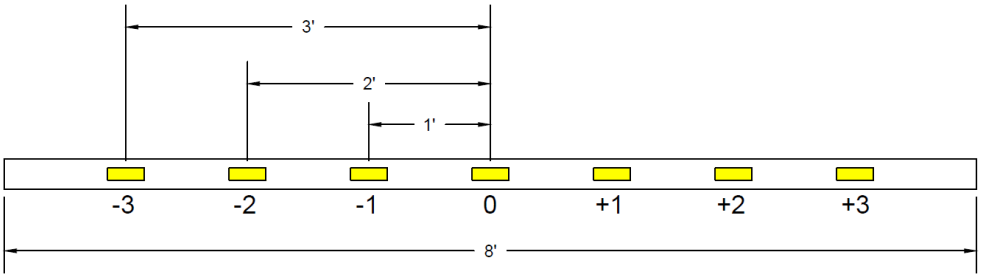

Figure 2.10: Series 2 - Station Layout

The purpose of Series 2 was to identify the effects of pressure variations for two nozzle sizes on pattern density. The pressures used represent the lower and upper limits of the suggested pressures for the nozzle type. The tests were organized as follows, with the altered variables listed in the table 2.1, all other variables were intended to be kept constant:

Table 2.1: Series 2 - Test Structure

Variable	Test 1	Test 2	Test 3	Test 4
Nozzle	XR8001	XR8001	XR8001	XR8001
Pressure (Bar)	1	2	3	4

	Test 5	Test 6	Test 7	Test 8
Nozzle	XR8002	XR8002	XR8002	XR8002
Pressure (Bar)	1	2	3	4

2.3.2 Series 3

Series 3 was intended to determine the full effective swath width of the UAS. This Series used a different spray analysis mechanism than the other tests. Instead of water sensitive paper, a cotton string designed to absorb a fluorescent dye, that would later be analyzed by a Fluorometer, was used. The purpose of this Series was to attempt to determine the full effective swath width of the UAS sprayer. This system did not gather information on individual droplets, but instead estimated droplet density based on string saturation. Each flight consisted of only one data station, but was repeated 3 times.

Table 2.2: Series 3 - Test Structure

	Test 1			Test 2		
Variable	Pass 1	Pass 2	Pass 3	Pass 1	Pass 2	Pass 3
Nozzle	XR8001	XR8001	XR8001	XR8002	XR8002	XR8002

2.3.3 Series 4

Test Series 4 was similar in layout to Series 2. The primary differences were the inclusion of the ODAQ described earlier, as well as recording the the flight using a single smartphone camera perpendicular to the flight path. This test was largely to replicate Series 2 with the inclusion of speed and height data which had not been collected the first time. Due to material limitations, the

3 bar test was omitted as the primary goal was to capture results from low and high pressures, interpolating the results in between, if necessary. Card spacing was increased to 0.6 m (2 ft) to encompass a wider area while still using fewer samples (Figure 2.11).

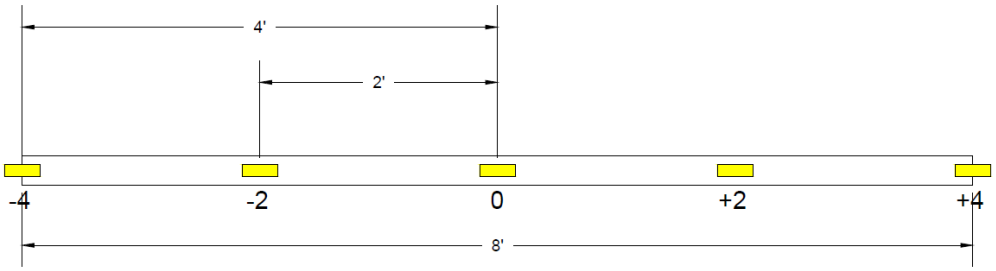

Figure 2.11: Series 4 - Station Layout

Table 2.3: Series 4 - Test Structure

Variable	Test 1	Test 2	Test 3	Test 4	Test 5	Test 6
Nozzle	XR8001	XR8001	XR8001	XR8002	XR8002	XR8002
Pressure (Bar)	1	2	4	1	2	4

2.3.4 Series 5

Test Series 5 altered the frame layout (Figure 2.13), removing one frame and decreasing the distance between the remaining two, in an attempt to capture redundant data at a single location (Figure 2.12). Since in prior tests, speed variation was accomplished by continuously accelerating through 3 evenly placed stations, this test instead changed the flight behavior to a method where half of the tests the UAS pitched forward at a shallow angle, providing a low acceleration, while pitching at a more aggressive angle for higher acceleration in the other half. The intention was to capture effects at much higher velocities than previous tests, and was the primary focus of Series 5. Test pressures were changed to 2-4 bar, excluding 1 bar due to observations from previous tests showing high sensitivity and difficulty in producing consistent densities and droplet sizes at this low of a pressure.

Card Spacing was returned to 0.3 m (1 ft) to increase the resolution of the spray pattern.

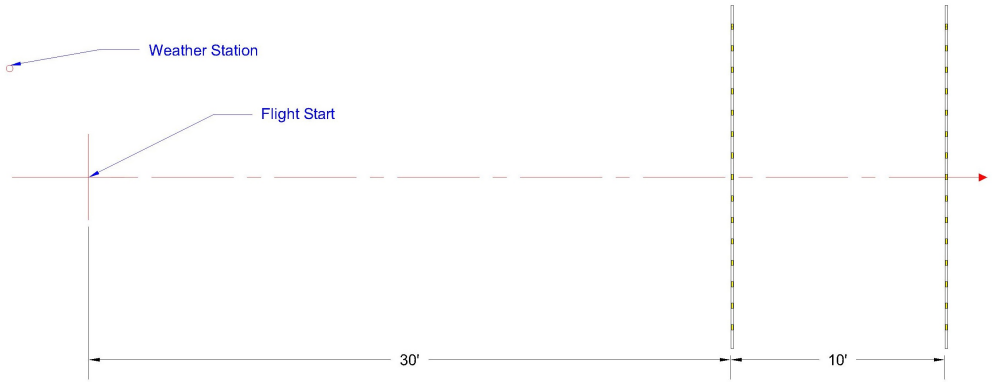

Figure 2.12: Series 5 - Test Layout

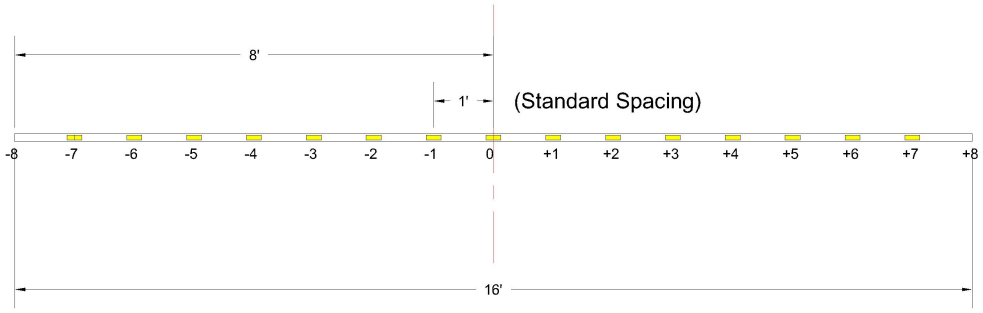

Figure 2.13: Series 5 - Station Layout

Table 2.4: Series 5 - Test Structure

Variable	Test 1	Test 2	Test 3	Test 4	Test 5	Test 6
Pressure (Bar)	2	3	4	2	3	4
Nozzle	XR8001	XR8001	XR8001	XR8002	XR8002	XR8002
Acceleration	Low	Low	Low	Low	Low	Low

Variable	Test 7	Test 8	Test 9	Test 10	Test 11	Test 12
Pressure (Bar)	2	3	4	2	3	4
Nozzle	XR8002	XR8002	XR8002	XR8001	XR8001	XR8001
Acceleration	High	High	High	High	High	High

2.3.5 Series 6

Test Series 6 attempted to determine the effects of variables not intentionally altered in previous tests, primarily flight height and nozzle type. Additionally, instead of focusing only on the spray pattern directly beneath the UAS as in Series 2 through 5, samples were collected on either side and above, in an attempt to determine the full pattern distribution within the vicinity of the UAS. Results from Series 2 and 5 indicated a potential loss of a significant amount of the spray pattern as well as uneven distribution, which would ideally be explained by capture of the entire pattern distribution using the enclosed frame design. Data collection stations consisted of PVC frames, constructed to support an evenly spaced array of water sensitive paper that would enclose the UAS from all sides as it passed through (Figure 2.14). Three stations were used for each pass and each station was adjustable, allowing for consistent offset of the water sensitive paper, as various application heights were tested. This system provided more complete insight into the entire distribution of the spray pattern. Station quantity and spacing were the same as in series 2 and 4.

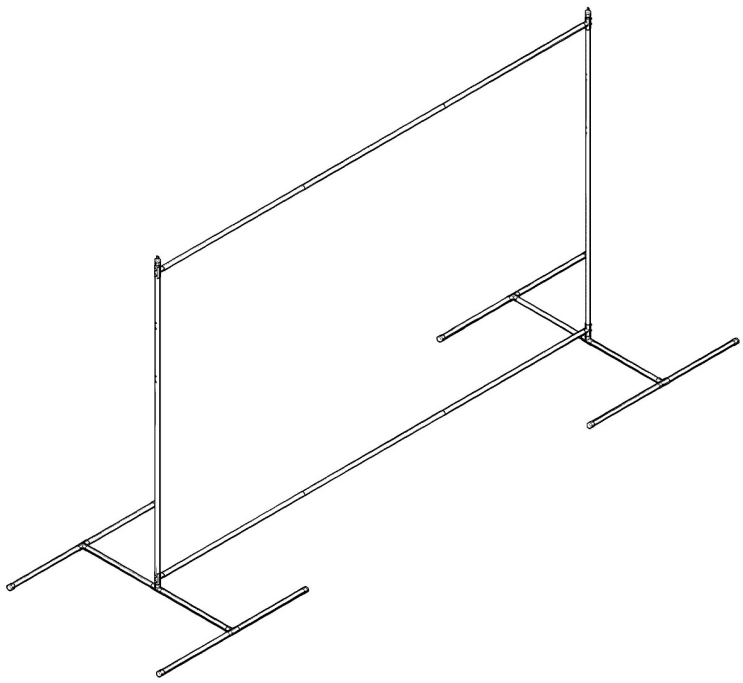

Figure 2.14: Series 6 - Frame Structure

Flight heights were based on the suggested application height for the 80°

nozzle. Four heights were used, the first being 50% the suggested height, second was the suggested height, third 150% the suggested height, and fourth 200%. It should be noted that the optimum spray height for 80° nozzles with the spacing used is approximately 0.76 m (30 in), but 0.5 m (20 in) for 110° nozzles.

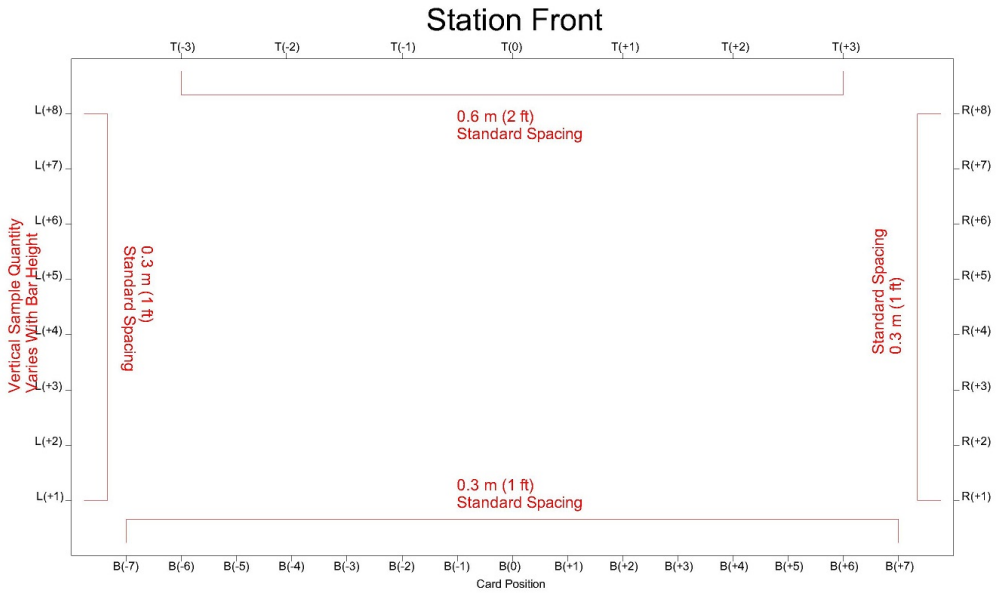

Figure 2.15: Series 6 - Sample Card Spacing

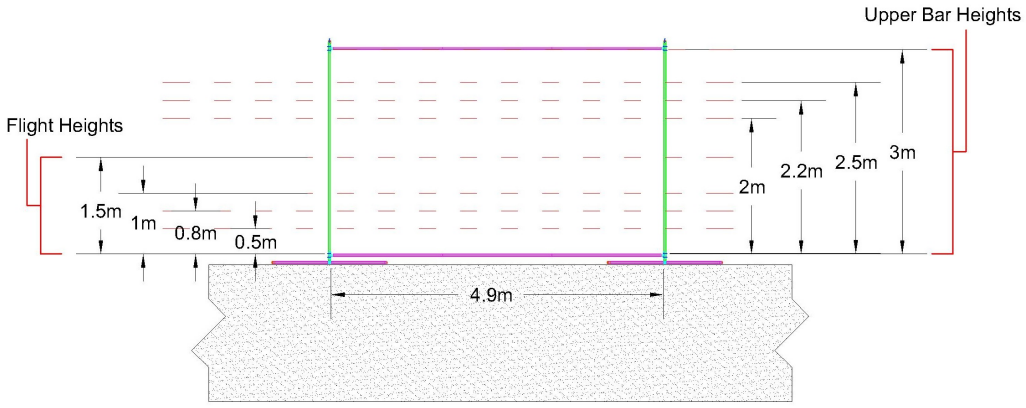

Figure 2.16: Series 6 - Frame Heights

For this Series, 01 nozzles were omitted based on results collected from previous tests regarding the droplet spectrum. This Series intended to expand on results already collected from previous tests, but the differences between

the XR 01 and 02 nozzles were not considered significant enough to warrant doubling the number of tests (especially due to material constraints). Additionally, the XR 01 nozzle showed higher sensitivity to environmental conditions, and therefore made the 02 nozzle a more logical choice for comparison between nozzle types, representing an upper bound for flow rate based on the selection criteria imposed earlier. The inclusion of the XR nozzle was largely to establish a base of comparison that could tie the results from previous Series to the results in Series 6. Effects of pressure variation were not included in this Series, so pressure was fixed at 2 bar, based on limiting the amount of small droplets produced [25] and also avoiding the lower end of the nozzle pressure range, where observations from previous tests showed high variability in droplet size.

Figure 2.17: Series 6 - Test Setup

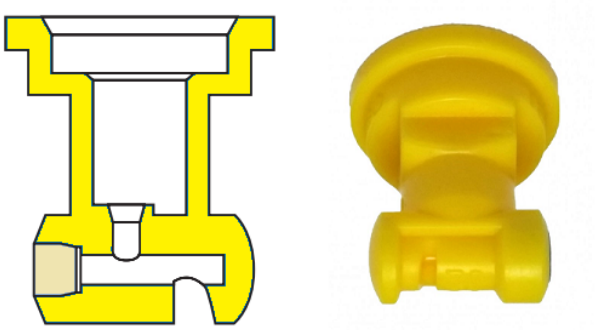

Figure 2.18: TeeJet TT Nozzle

TT (Turbo TeeJet) nozzles are also flat fan nozzles, but contain a pre-orifice. The pre-orifice meters fluid flow prior to the formation of droplets,

altering the pattern characteristics. In this case the result is a droplet spectrum shifted toward larger droplets than those from the XR nozzle [25].

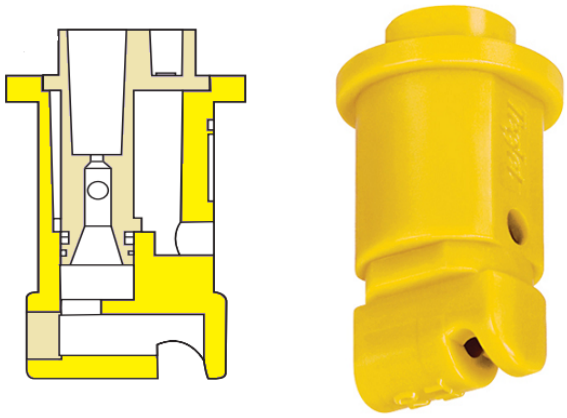

Figure 2.19: TeeJet TTI Nozzle

The TTI (Turbo TeeJet Induction) contains similar design features to the TT nozzle with the addition of air induction. A Venturi air aspirated chamber creates air bubbles inside droplets as well as causing droplets to coalesce to form a significantly larger droplet spectrum, with droplets in the Ultra Coarse and Extremely Coarse range while decreasing the pattern density [25].

Table 2.5: Series 6 - Test Structure

	Test 1			
Variable	Pass 1	Pass 2	Pass 3	Pass 4
Nozzle	XR8002	XR8002	XR8002	XR8002
Height (m)	0.5	1	0.8	1.5

	Test 2			
Variable	Pass 1	Pass 2	Pass 3	Pass 4
Nozzle	TT11002	TT11002	TT11002	TT11002
Height (m)	0.5	0.8	1	1.5

	Test 3			
Variable	Pass 1	Pass 2	Pass 3	Pass 4
Nozzle	TTI11002	TTI11002	TTI11002	TTI11002
Height (m)	1.5	1	0.8	0.5

2.4 Analysis Methods

The data compilation process for the droplet pattern tests (Series 2,4,5, and 6) relied primarily on the previously described droplet analysis programs to produce values which represented each sample card (Figure 2.9). Sample cards were scanned, and then each droplet was tallied recording sizes and quantities. These values were then used to compute a range of values for each card.

VMD (also DV5) - Sorting all detected droplets from smallest to largest, then summing the droplet volume beginning at the smallest droplet, this represents the droplet size when 50% of the total volume deposited on the card, is reached. Can be viewed as an average droplet size value. Similar measurements are taken to estimate the typical small (DV1 or 10% volume) and large (DV9 or 90% volume) droplet sizes, providing insight into the uniformity of the droplet spectrum.

Density (drop/cm^2) - Represents the average droplet density and is often used to assess the effectiveness of a spray pattern. Syngenta provides general

recommendations for pattern density based on pesticide type and typical chemical dilution [26]. These values were displayed as thresholds on several plots to provide a reference, but were not intended as a gauge of application quality, since they are specific to common application systems and standards.

Deposition (uL/cm^2) - Represents an estimate of the fluid volume deposited on a region based on droplet size. When compared to density can provide insight into the size of the droplets. These values were excluded from the Matlab droplet detection program (and hence Series 6) as this information is assessed through the DV values.

It is important to note that while these results are useful in the scope of this project and for comparison to results obtained through similar methods, comparison of pattern characteristics such as VMD to those obtained via methods such as the use of laser droplet sampling in a laboratory setting could potentially yield varying results, as an identical spray pattern may undergo fairly significant changes between formation and deposit especially with the inclusion of realistic environmental conditions [27]. Comparison to results collected in laboratory conditions, and provided by the nozzle manufacturer, are made to provide a basis of comparison but not intended to identify deviations in pattern behavior. The primary purpose for obtaining these values was comparison between test series. For estimation of environmental effects on droplet characteristics, refer back to Section 1.2.

For this project, all height, velocity and position measurements (when taken) were made by using cameras. Videos were recorded at 30 fps allowing fairly accurate velocity measurement (approximately $\pm$ 0.1 m/s) by measuring the travel distance over a set number of frames and scaling images to frame component sizes in the vicinity of the UAS. The scaled images were then also used to estimate height and lateral position (approximately $\pm$ 0.1 m).

CHAPTER 3

RESULTS

3.1 Presentation of Data

Figure 3.1 is a sample diagram of the results from a single test station. This specific diagram is taken from Series 6, so some of the elements may not be used in diagrams from prior tests.

The title indicates the Series number, followed by the Test, the Pass, the Station and the nozzle type. This diagram is oriented so that it represents the view of the Station frame as the UAS is flying away from the operator.

Borders surrounding the plots represent each surface of the frame interior, Series 6 is the only one with side and top borders representing surfaces.

The blue shaded area represents the coverage density at every sample card, with a scale on the left side of the diagram. Typical droplet density recommendations provided by Syngenta are labeled as the PostE-Herbicides (Post-Emergence Herbicides) and Insecticide/PreE-Herbicides (Pre-Emergence Herbicides) thresholds. These are included simply for reference and were not used as a metric to gauge application quality in this project. (Note: Refer to Figure 3.1 for identification of underlined items in the following description)

- Tick marks indicate a water-sensitive paper sample card location.
- Colored circles indicate the VMD at that sample card, with the color and diameter corresponding to the ASABE standard for droplet size classification, shown previously in Figure 2.7.
- The green bar near the center of the plots represents the UAS, its flight height and lateral position, as well as Nozzle Spray Angle and nozzle angle offset, being indicated directly beneath (in the yellow hatched area). UAS velocity is indicated next to the icon.

- The red arrow identifies compass North relative to the Station, where up corresponds to the same flight direction as the UAS (away from the operator).

- The table on the left contains UAS Data with respect to the flight characteristics as the UAS passes the station. The bottom row contains Weather Data information at that time.

- The Wind Table contains a record of the wind speed and direction before, during, and after the UAS passes the station (as indicated by positive and negative time stamps). Wind speed and direction recordings took approximately 2 seconds, and as a result were in the same order of magnitude as the entire flight duration. Since droplet settling time varies with size (see explanation in Section 1.2), and to illustrate wind trends around the time of spraying, wind was recorded for periods prior to, and after the UAS passed each station.

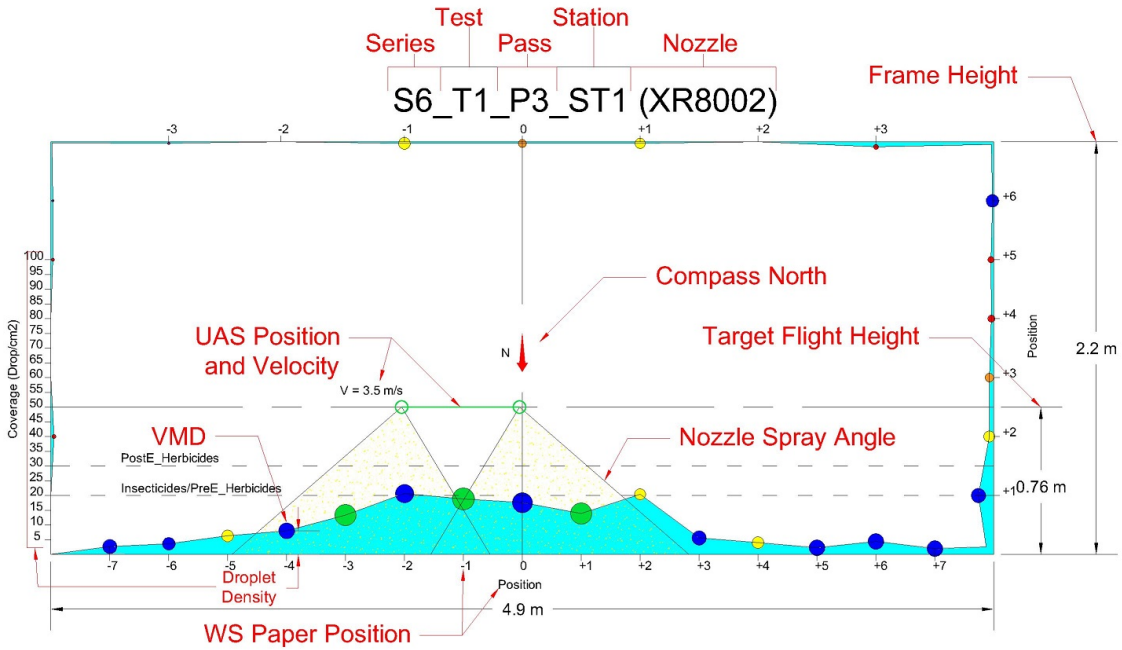

UAS Data

Height (m)	Lat. Position (m)	Velocity (m/s)	Sys. Pressure (Bar)
0.8	-0.32	3.5	2

Weather Data

Temperature (C)	Humidity (RH)	Barometric Pressure (Pa)	
15.8	51.15	99660	

Wind Table

Time	Wind Speed	Wind Direction
NA	NA	NA
-2.62	NA	NA
0.00	1.3	N
2.62	1.3	S
5.23	1.7	NW

T_0 UAS@Station

Figure 3.1: Sample Station Diagram

3.2 Test Results

3.2.1 Series 2

Series 2 and 4 were again focused on establishing the results of variation of pressure and flow rate. Results from Series 2 displayed significantly more variation in the VMD than indicated by the nozzle data sheets. VMD for both the XR8001 and XR8002 is primarily in the Fine spectrum (136-177 micron) with the lowest pressure for the 02 nozzle entering the Medium spectrum (177-218 micron). However, the sampled VMD at lowest pressures for 01 nozzle was in the Very Coarse spectrum (349-428 micron), as seen in Figure 3.2, and the 02 nozzle was in the Very Coarse and Coarse spectrum (218-349 micron), as seen in Figure 3.3.

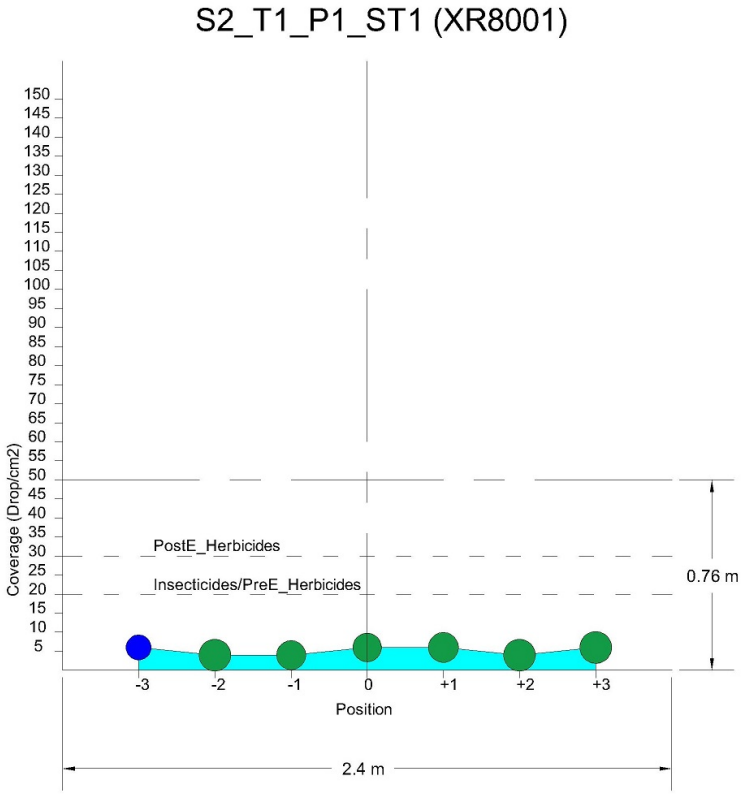

Figure 3.2: Series 2 - Typical XR8001 Pattern

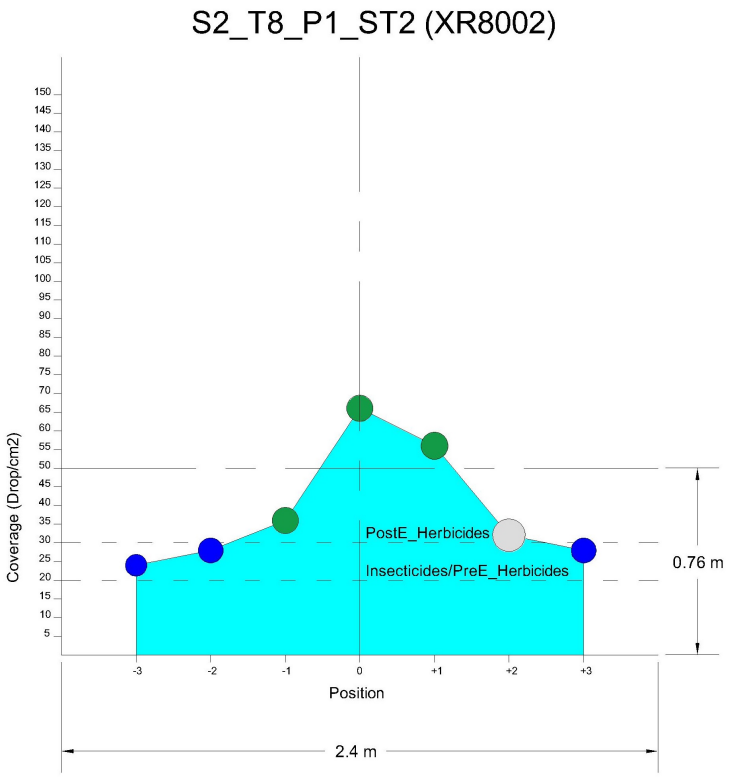

Figure 3.3: Series 2 - Typical XR8002 Pattern

The following plots illustrate a comparison of pattern characteristics with respect to flow rate, in order to determine if the spray pattern follows predicted trends as pressure increased. From Figure 3.10 it can be observed that both volume and pattern density increase fairly linearly with pressure increases (flow rate) for the 02 nozzle, which match the predicted behavior of the XR nozzle. However, the 01 nozzle instead displays a drop in volume with a sharp increase in density in Figure 3.4.

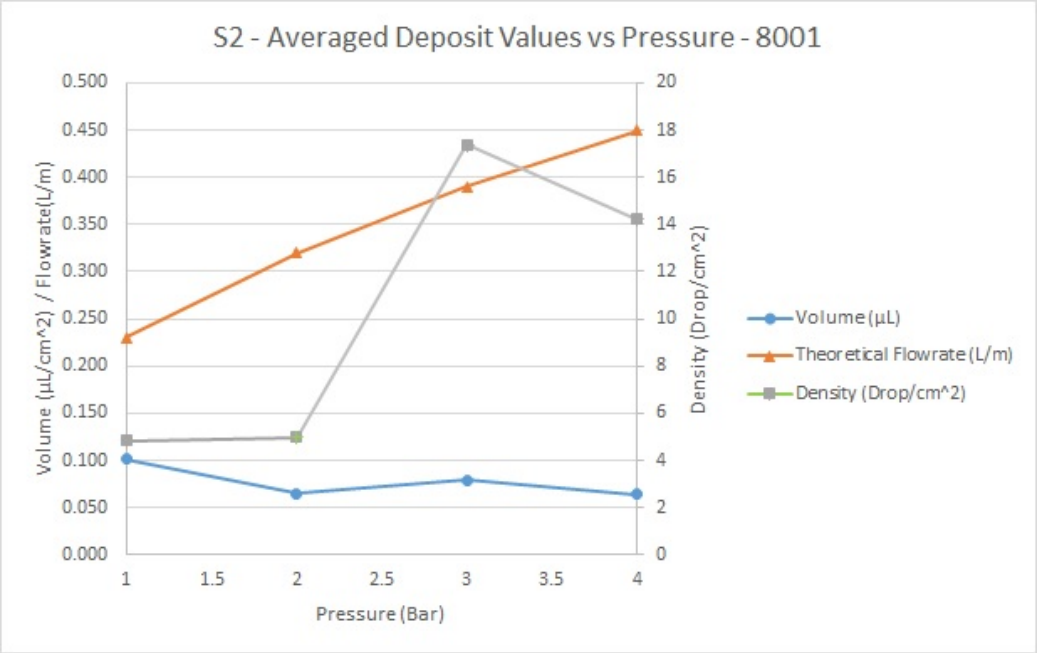

Figure 3.4: Series 2 - Comparison of Pressure and Deposit Volume for XR8001

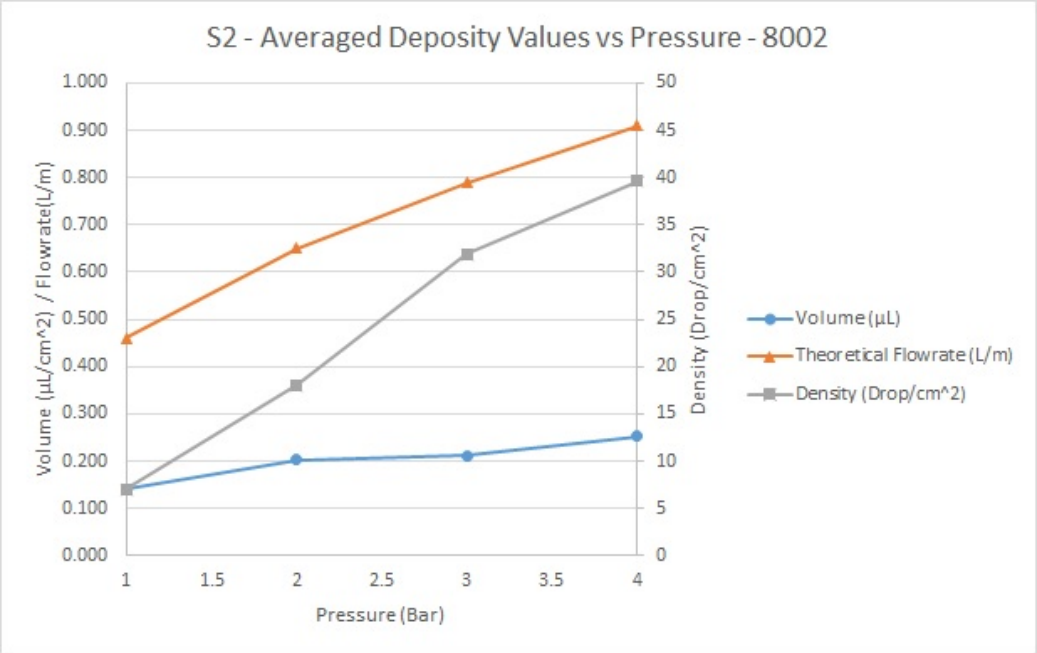

Figure 3.5: Series 2 - Comparison of Pressure and Deposit Volume for XR8002

A correlation matrix was used as a simple method to quickly identify major influencing factors from the test data, as tests were numerous as was

the amount of data collected. These influencing factors are then plotted to visualize the trend and further assess its behavior. The correlation matrix identifies linear relationships between variables. It is symmetric and establishes relationships between variables via Equation 3.1:

$$\rho_{ij} = \frac{\sigma_{ij}}{\sqrt{\sigma_{ii}\sigma_{jj}}} \tag{3.1}$$

Where σ is the standard deviation, ρ is the correlation coefficient and, i and j are the row and column position respectively. Table 3.1 for Series 2 is the output of a correlation matrix comparing the spray pattern characteristics to the operation parameters selected for the UAS. The output utilized data from all tests from Series 2. The values in the cells indicate the linear association, with 1 being the highest possible value (which is why variables compared to themselves all have a value of 1) and 0 suggesting independence. Positive and negative values indicate the slope of the trend line. It should be noted that since this method is only valid for linear relationships it cannot be assumed that uncorrelated variables are not related at all, it's simply a method of identifying relationships that warrant further analysis [28].

While the individual station diagrams described in Section 3.1 are useful to visualize what the results actually look like, the data gained from a single station is not sufficient to make any conclusions, and they are simply used to demonstrate an example of the findings of the correlation matrices and plots. All station diagrams and weather data collected are available in the appendix.

Table 3.1: Series 2 Correlation Matrix and Key

	A	B	C	D	E	F	G
A	1	0.56	-0.44	-0.17	0.1	0.88	0.85
B	0.56	1	-0.84	-0.75	0.56	0.68	0.19
C	-0.44	-0.84	1	0.87	0.58	-0.6	-0.07
D	-0.17	-0.75	0.87	1	0.84	-0.36	0.19
E	0.1	-0.56	0.58	0.84	1	-0.09	0.43
F	0.88	0.68	-0.6	-0.36	0.09	1	0.77
G	0.85	0.19	-0.07	0.19	0.43	0.77	1

A	B	C	D	E	F	G
Flow Rate	Pressure	DV1	DV5	DV9	Density	Deposit Volume

Since relatively few flight parameters were recorded for this test Series, this first matrix primarily can be used to verify the spray distribution behaves as expected with the given inputs. Some observations include:

- A strong positive correlation between pressure/flow rate and deposit volume and density. Flow rate is a variable taken from the table of nozzle characteristics, for each nozzle, and is pressure dependent. The only reason they are not correlated at a value of 1 is due to the fact that the 01 and 02 nozzles produce different flow rates at the same pressures, because of orifice size.

- A strong negative correlation between DV and pressure. As pressure increases with the tested nozzles, droplet size decreases, this indicates the spray pattern generally followed the expected behavior. Increasing pressure had a much stronger influence on the DV1 droplet diameter (generally the smallest droplets in the spectrum) than DV5 or DV9. Implying droplets representing the lowest 10% experienced a more significant shift than the larger 90%.

3.2.2 Series 3

Effective swath width is determined by assessing the peak density of a spray pattern, locating the edges of the trapezoid formed by the spray pattern and taking the measurement between the locations where the density is 50% of the peak (Figure 3.6).

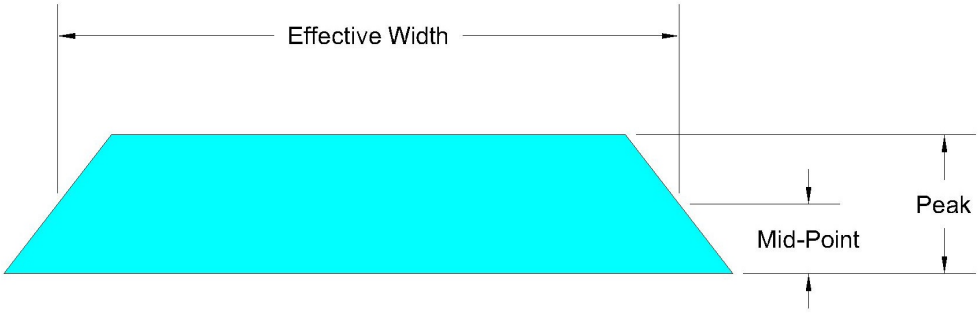

Figure 3.6: Estimation of Effective Swath Width

Analysis of the spray pattern from Test 1 consisted of averaging deposit values from the 3 passes to estimate the true pattern width. Figure 3.7 shows results from the 3 passes, superimposed into a single plot, and then the average result below, where the peak is indicated in the top plot and the midpoint in the bottom plot. Estimated swath width from this test was approximately 4.5 m which is over double what would be expected for this nozzle configuration (approximately 1.5 m). A slight right nozzle bias can be seen in the averaged pattern, indicating possible variation in the nozzle flow rate due to an issue with the spray system. The test was intentionally carried out parallel to the wind direction, and for the most part these conditions remained constant (which can be referenced in the appendix files), so it is not as likely to be an explanation for this bias.

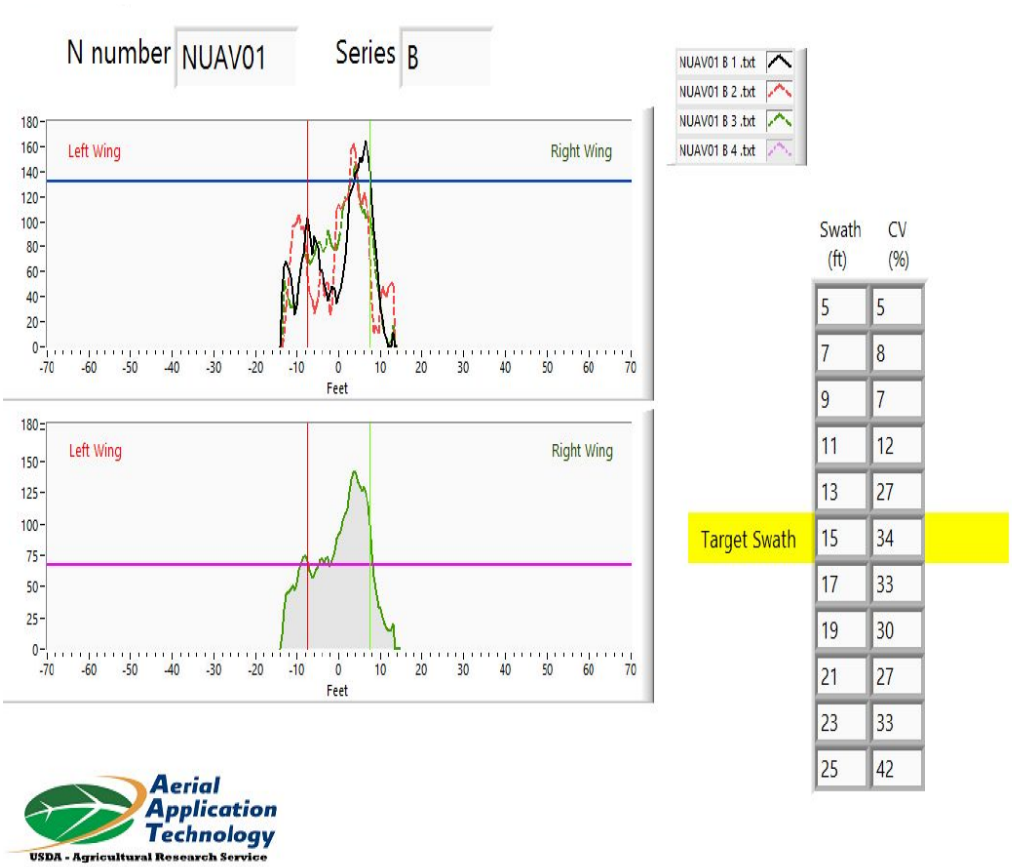

Figure 3.7: Series 3 - XR8001 Pattern Width Estimation

Test 2 produced the same effective swath width, with a CV similar to Test 1, however the pattern appeared to show less bias toward the right side as can be seen in Figure 3.8. This test provided valuable insight into how large the actual effective pattern width could be for this nozzle, and prompted the increase in testing width for the later Series.

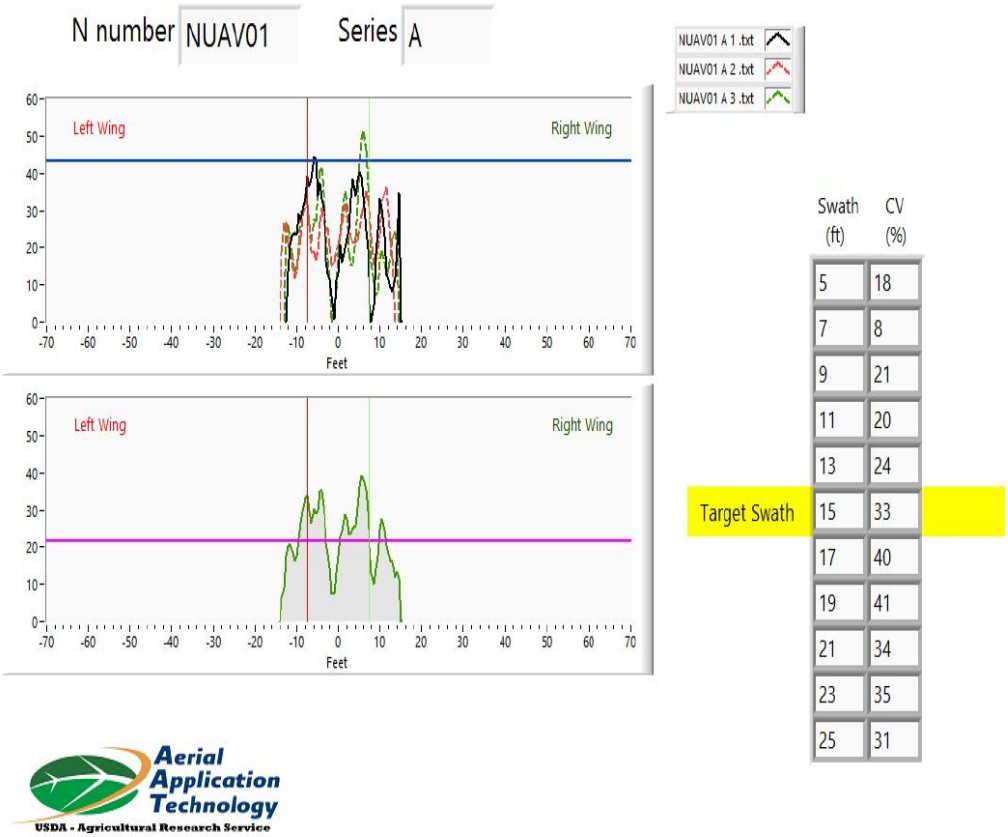

Figure 3.8: Series 3 - XR8002 Pattern Width Estimation

3.2.3 Series 4

Table 3.2 is the correlation matrix from Series 4. Inclusion of more recorded flight parameters increased the matrix size, so labels were assigned to single letters, the key can be referenced below the table.

Table 3.2: Series 4 Correlation Matrix

	A	B	C	D	E	F	G	H	I	J	K	L
A	1	0.61	0.22	-0.51	0.27	-0.41	-0.73	-0.18	-0.18	-0.27	0.77	0.84
B	0.61	1	0.42	-0.39	-0.39	0.26	-0.62	-0.72	-0.64	-0.58	0.78	0.32
C	0.22	0.42	1	-0.61	-0.34	0.27	-0.36	-0.25	-0.41	-0.34	0.34	0.20
D	-0.51	-0.39	-0.61	1	0.27	-0.17	0.69	0.08	0.15	0.07	-0.48	-0.55
E	0.27	-0.39	-0.34	0.27	1	-0.96	0.35	0.44	0.34	0.13	-0.01	0.42
F	-0.41	0.26	0.27	-0.17	-0.96	1	-0.24	-0.47	-0.33	-0.08	-0.07	-0.50
G	-0.73	-0.62	-0.36	0.69	0.35	-0.24	1	0.35	0.25	0.18	-0.63	-0.55
H	-0.18	-0.72	-0.25	0.08	0.44	-0.47	0.35	1	0.89	0.75	-0.53	0.11
I	-0.18	-0.64	-0.41	0.15	0.34	-0.33	0.25	0.89	1	0.92	-0.42	0.12
J	-0.27	-0.58	-0.34	0.07	0.13	-0.08	0.18	0.75	0.92	1	-0.40	0.04
K	0.77	0.78	0.34	-0.48	-0.01	-0.07	-0.63	-0.53	-0.42	-0.40	1	0.73
L	0.84	0.32	0.20	-0.55	0.42	-0.50	-0.55	0.11	0.12	0.04	0.73	1

A	B	C	D	E	F
Flow Rate	Pressure	Height	Velocity	Temperature	Humidity

G	H	I	J	K	L
Barometric Pressure	DV1	DV5	DV9	Density	Deposit Volume

Observations on the matrix are as follows:

- As seen in Series 2, there was a strong positive correlation between pressure/flow rate and deposit volume and density.
- Also seen from Series 2, a strong negative correlation between DV and pressure.
- Height and velocity were fairly strongly correlated, so correlations for either will appear for both. However, as height was not intentionally varied, the range is only over about 0.2 m for all tests, while velocity varies by closer to 4 m/s. The implication being that pattern effects correlated to either, are more likely correlated to velocity.
- A moderate negative correlation between velocity and density, implying increased velocities result in lower application densities, which is to be expected.

Comparison of pattern characteristics to estimated flow rate provided results similar to Series 2. The 01 nozzle in Figure 3.9 shows the same increase in density with the flow rate, while volume again drops. The 02 nozzle in Figure 3.10 shows an increase in both variables with flow rate. As the nozzle specifications suggest and as the correlation matrices from Series 2 and 4 confirm, the pattern DV values decrease significantly as pressure is increased, with the greatest effect being on the DV1 values, implying a significant shift in the characteristics or quantity of very small droplets. This corresponds to the manufacturer's laboratory analysis of the XR nozzle, suggesting 19% of droplets are under 150 micron at 1.5 bar and 30% under 150 micron at 3 bar for an 03 nozzle [25]. These values would be higher for an 02 and especially an 01 nozzle. Due to these droplets sensitivity to airflow, a significant portion of the spray volume could have been deposited outside the

target area as a result of the UAS downwash or wind. While the variation in VMD could also be attributed to the difference in testing methods between laboratory analysis and field analysis mentioned earlier, this offers a more plausible explanation and highlights the importance of the testing methods used in Series 6.

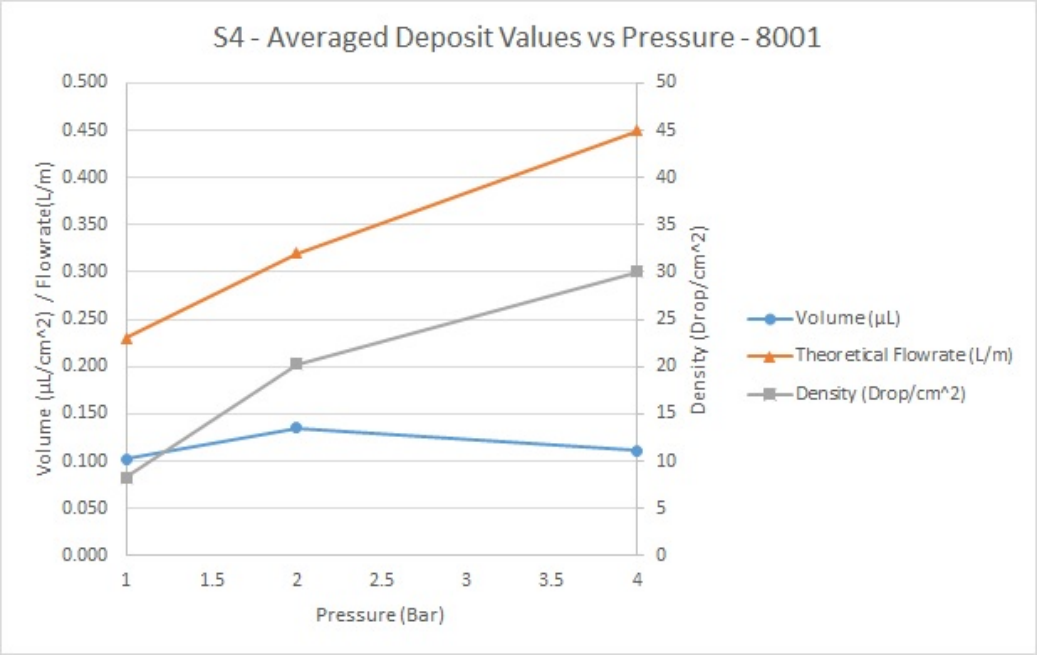

Figure 3.9: Series 4 - Comparison of Pressure and Deposit Volume for XR8001

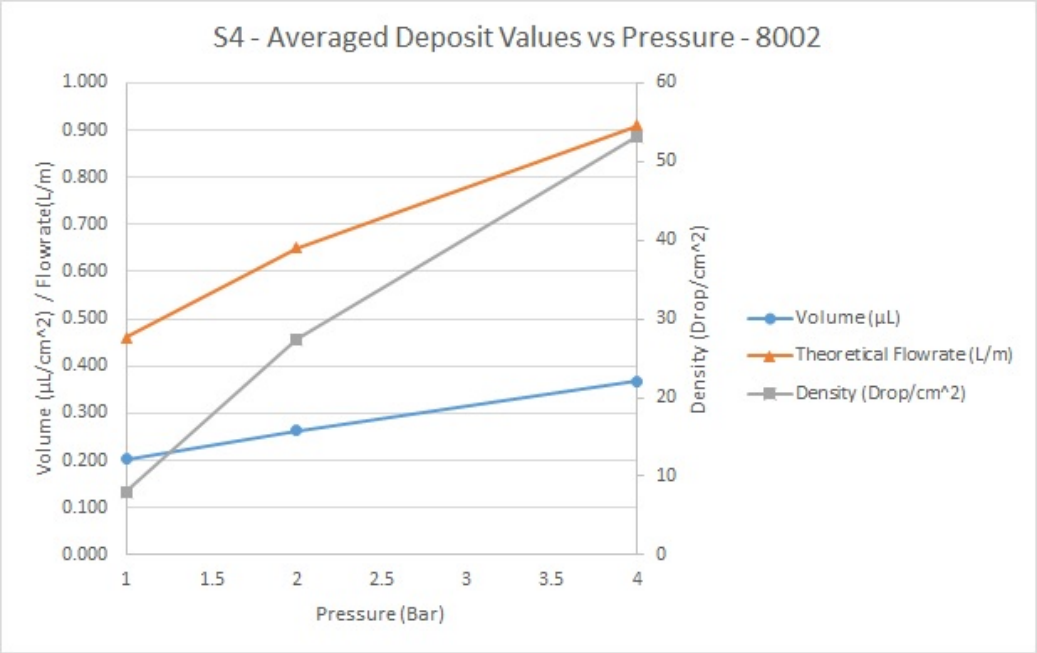

Figure 3.10: Series 4 - Comparison of Pressure and Deposit Volume for XR8002

3.2.4 Series 5

Series 5 and 6 did not include the fluorometer and string for spray pattern width estimation, but pattern width was still estimated through droplet density on the water-sensitive paper, since the paper extended beyond the original effective swath width found in Series 3. The swath width was estimated via the same method mentioned in Series 3. Additionally a pattern center was estimated by calculating the midpoint of the distribution based on coverage density. Finally, CV was included for each pattern, obtained from Equation 3.2:

$$CV = 100\frac{\sigma}{\mu} \tag{3.2}$$

Where σ is the standard deviation and μ is the mean.

In order to include variables in the correlation matrix, only a single number can be used. Since wind was observed over a period of time and every station contained several observations, the reading that corresponded to the pattern shift relative to the UAS (if one was apparent) was selected. The focus of velocity variation in Series 5 seemed to result in some changes in the observed

correlations:

- Seen from previous tests, confirmation of a strong positive correlation between pressure/flow rate and deposit volume and density.
- In addition to other characteristics, a relation between nozzle flow rate and pattern width is also apparent. For certain nozzles, spray pressure can influence the effective pattern width. A standard example of a 11002 nozzle producing a 90° spray pattern at a very low pressure (1 bar) and increasing to the designed angle of 110° at 3 bar [25].
- Due to the testing style involving very aggressive flying for the higher velocity tests, height and velocity were strongly correlated, and as a result, their separate effects are difficult to distinguish. The same assumption regarding height made in Series 4 should not be made here, as height varied by almost 1 m vs the 0.2 m seen in Series 4.
- Both wind direction and lateral position had strong correlation to the position of the pattern center, with position being slightly stronger. Wind direction also was more strongly related to the center deviation, which is to be expected.
- Pattern center and center deviation were strongly correlated.
- Values from pattern characteristics assessed within the effective swath width (density, CV, deposit volume) will be correlated to other pattern characteristics (off-target %, pattern width), since evaluation of these variables inherently involves inclusion of the others. This is true for Series 6 as well.

The aggressive variation acceleration (and hence flight speeds at stations) provided a larger range of speed data than that contained in previous tests, as a result a clear trend could be observed between flight speed and pattern deposit values (Figure 3.11). Most notably, this plot and the findings in the correlation matrix

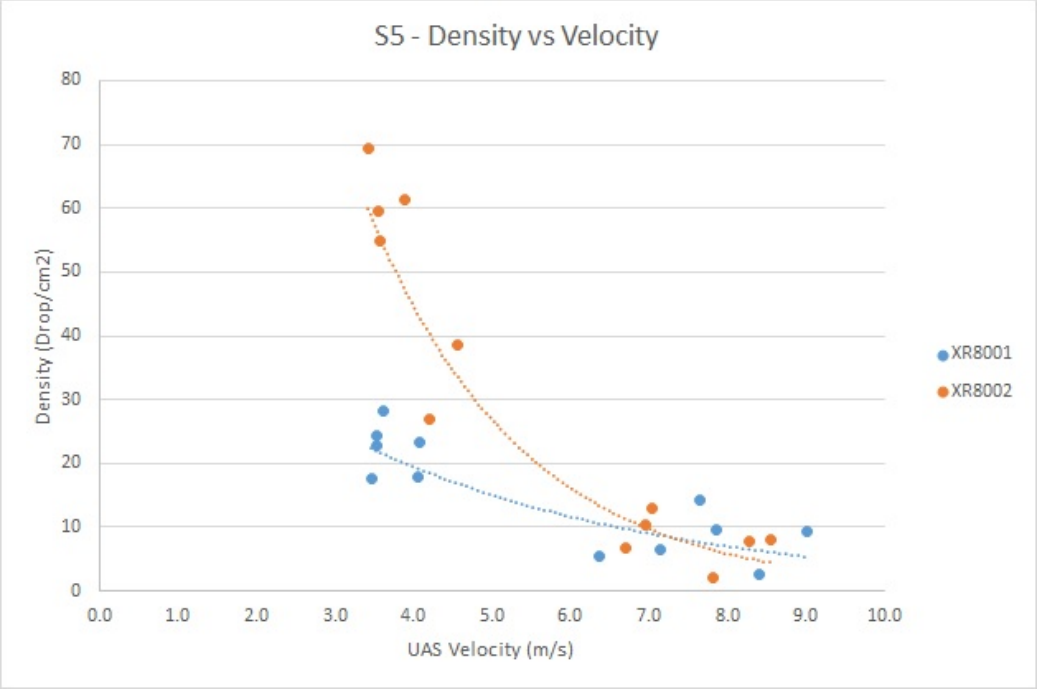

Figure 3.11: Series 5 - Comparison of UAS Velocity and Density

What this seems to indicate, is that regardless of doubling of flow rate, velocities excessive enough (7-9 m/s (15-20 mph)) would result in similarly low application densities.

3.2.5 Series 6

Effective swath width, pattern center and CV were characterized via the same methods mentioned in Series 5, with the addition of the variable Off-Target %. As the intent of Series 6 was to determine the full distribution of the spray pattern, this variable subtracted the total density of the effective swath width from the total recorded density over the entire frame and determined off-target spray as any spray outside the effective width.

The following observations were made from the analysis of four correlation matrices (which have been included in the appendix). With Series 6 focusing on height variation and variation of nozzle type, more information was gained by expanding the number of matrices produced, to also remove the overarching effect of the nozzle type. The first matrix combined all data from the three tests and the observations are listed below, those following only included data from individual Tests and are labeled as such:

General (Combined Nozzle Data)

- A fairly weak negative correlation, relative to other correlations, was noted between velocity and density. This however, was still the strongest correlation for velocity.
- In all three tests, velocity was heavily correlated with pattern width, pattern center and center deviation. There is also a strong correlation between pattern center and velocity, which makes differentiation difficult. Pattern center is more likely to explain center deviation than velocity.
- Many of the correlations between variables that are not the nozzle type are more apparent in independent nozzle tests, as nozzle type is one of the strongest influencing variables in this matrix.
- Weather (mostly temperature and humidity) varied fairly significantly by test date. Since each nozzle was tested in a single day, weather effects in this correlation matrix are more likely to be effects from nozzle variation.

XR8002

- Very strong correlations between height and density, pattern width, pattern center, center deviation, and off-target application. Off-target % is mostly strongly influenced by height over all other input variables.
- Velocity is strongly correlated to lateral position, in this test as well, again implying some subjective differentiation is required when a strong correlation is found between them and any other variable. Velocity variation was relatively low compared to previous Series, so it is more likely this is not the influencing factor.
- A strong relation between DV1 and temperature, this could be partially due to evaporation rates of small droplets being sensitive to weather conditions, but also may be related to temperature changing throughout the testing period (in which flight heights were changed as well).
- A moderate correlation between wind speed and DV1, explained by small droplets being very sensitive to wind.

- Off-target application is correlated strongly with DV values and density largely because of the way they are assessed. DV values are only for droplets within the effective width, so when a significant amount (mostly small droplets) are blown off-target, the DV shifts.

TT11002

- Height and wind speed were strongly correlated, all variables correlated to these must be subjectively distinguished.

- Strong correlation between wind direction, pattern width, and density but these variables were also correlated with height. This is apparent in the XR and TT tests, which contained larger amounts of small droplets, but the same behavior was not observed in Series 5. Based on analysis of the plots produced by these tests, pattern width seems most logically associated with height. Based on previous results, height and wind direction both seem to be influencers of pattern density (noting again density is only measured in the effective swath width).

TTI11002

- Correlation between weather and DV1 seen in other two tests, is absent. This is likely due to relatively small amount of small droplets produced by this nozzle. Again referencing the previous analysis of small droplet behavior based on environmental conditions in Section 1.2.

- Height was strongly correlated to environmental conditions, so again subjective differentiation between other correlated variables is necessary when analyzing either.

- Pattern density was highly correlated to wind direction and height. However, given low wind speed values and low off-target application values (implying density did not decrease due to off-target application) it is more likely that height was the primary influencer in this case, as was the case with the previous nozzles.

Table 3.3 lists the theoretical pattern width of 80° and 110° nozzles at various heights provided by the nozzle manufacturer [25].

Table 3.3: Estimated Pattern Width vs Height

	Estimated Coverage Width (m)							
Height (m)	0.2	0.3	0.4	0.5	0.6	0.7	0.8	0.9
80°	0.3	0.5	0.7	0.8	1	1.2	1.3	1.5
110°	0.6	0.9	1.1	1.4	1.7	2	2.3	2.6

Observed spray pattern behaviors for the XR, TT and TTI nozzles, when compared to the values in Table 3.3 showed a similar trend to theoretical values (Figure 3.12). XR and TT nozzles generally followed the expected trends (the offset is due to using 2 nozzles for the UAS tests) with the XR nozzle deviating slightly in the positive direction as height increased. The TTI nozzle however changes very little with height, likely due to the effect of gravity on the larger droplets relative to their velocity upon exiting the nozzle orifice, as discussed in Section 1.2.

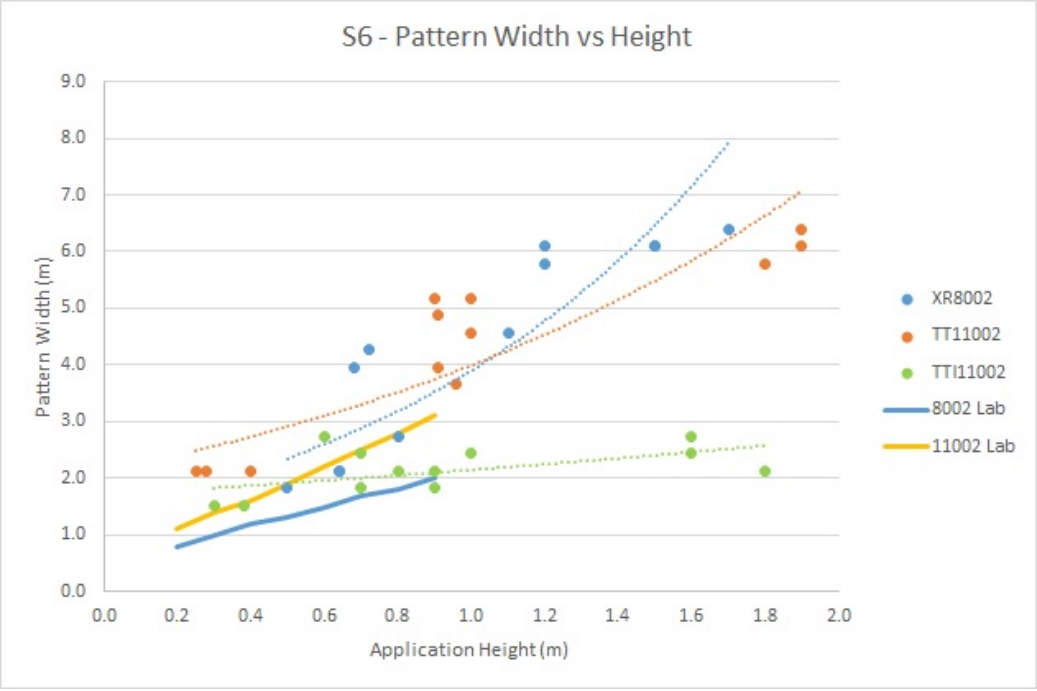

Figure 3.12: Series 6 - Comparison of UAS Height and Pattern Width

Manufacturer values for nozzle densities are not available in any format aside from coverage rates (L/ha (GPA)) relative to speed, but these numbers

can be compared effectively regardless in Figure 3.13. The XR nozzle produces higher density values at low heights, due to the large number of small droplets produced by the nozzle, but as height increases the density decreases drastically as these same droplets are much more sensitive to shifts in wind patterns, which is demonstrated in Figure 3.14 showing the percentage of off-target application. A typical example of this distribution can be seen in Figure 3.17. The TT nozzle showed a more uniform decrease, with a greater density at the greatest application heights.

Typically considered to be most at risk for drift, droplets below 150 micron make up a significant portion of the spray volume of the XR nozzle at (19% at 1.5 bar, 30% at 3 bar), while only accounting for a small portion of the TT nozzle (4% at 1.5 bar, 13% at 3 bar), with the volume being significantly lower (<1% at 1.5 bar, 3% at 3 bar) for the TTI nozzle [25]. The drastic difference in the TTI nozzles droplet spectrum (Extremely Coarse to Ultra Coarse) and resulting density decrease is apparent in Figures 3.20 and 3.19, where there is very little change in the pattern relative to the other two nozzles.

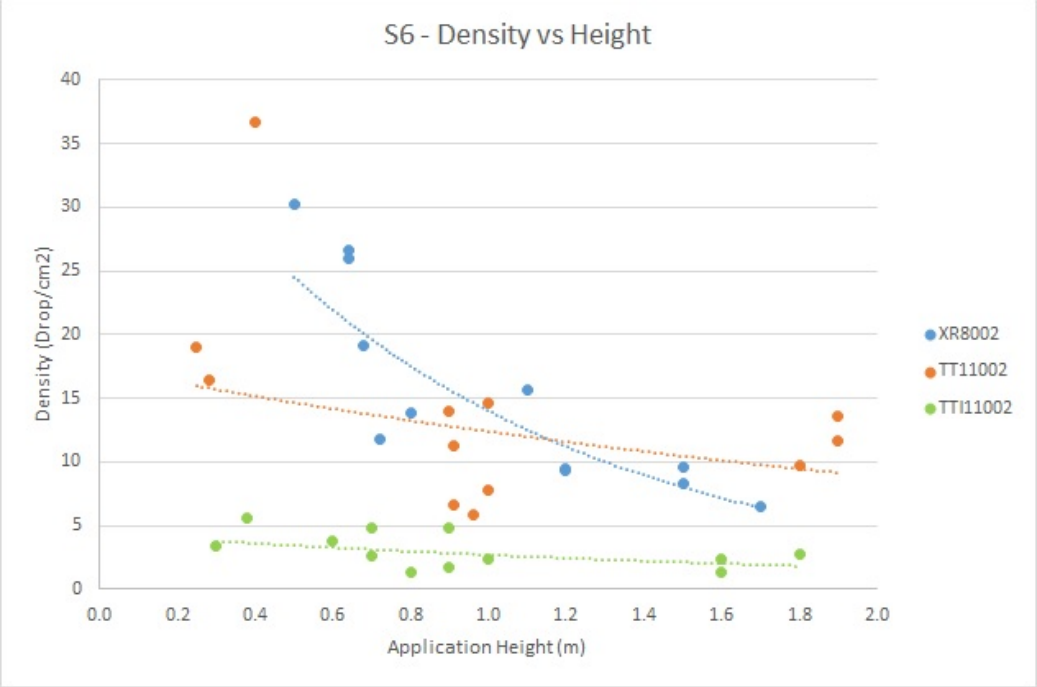

Figure 3.13: Series 6 - Comparison of UAS Height and Pattern Density

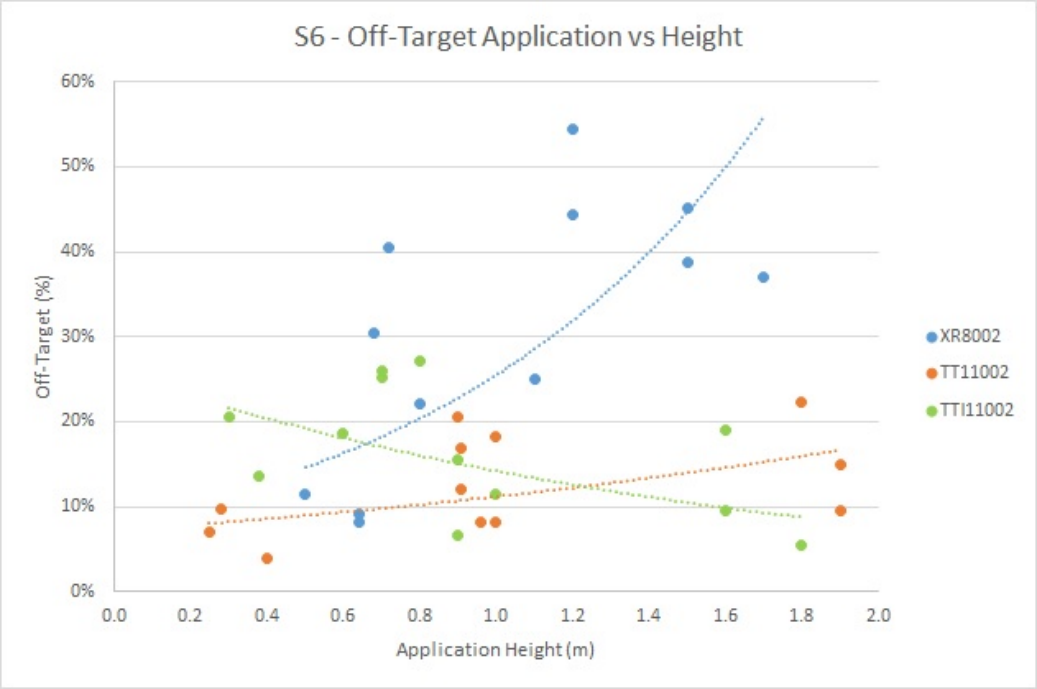

Figure 3.14: Series 6 - Comparison of UAS Height and Off-Target Application

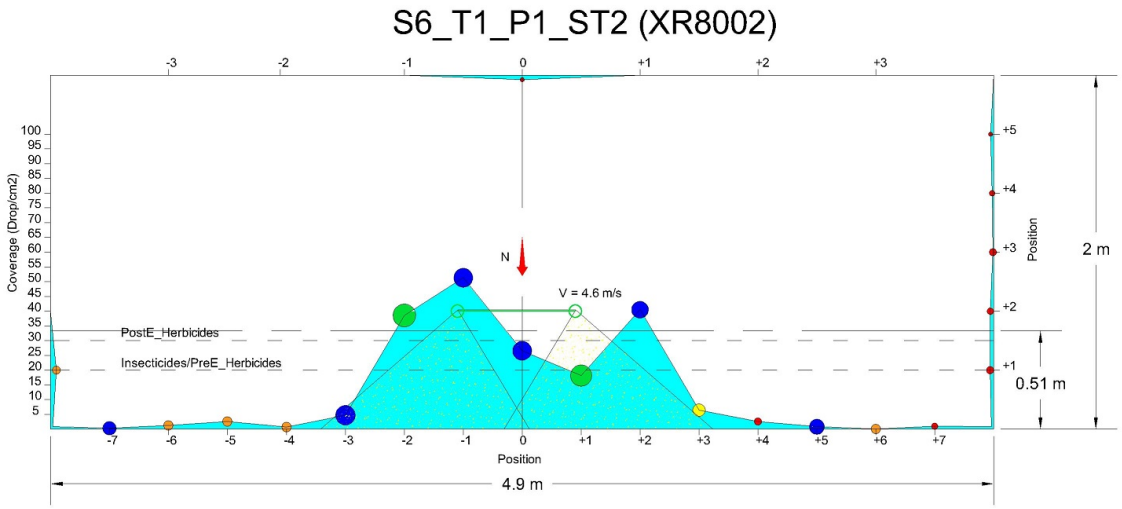

Height (m)	Lat. Position (m)	Velocity (m/s)	Sys. Pressure (Bar)
0.64	-0.02	4.6	2
Temperature (C)	Humidity (RH)	Barometric Pressure (Pa)	
19.58	45.04	99259	

Time	Wind Speed	Wind Direction
-5.23	2.3	S
-2.62	2.0	S
0.00	2.0	SW
2.62	2.3	S
5.23	2.6	S

Figure 3.15: Series 6 - Test 1 - Pass 1 - Station 2

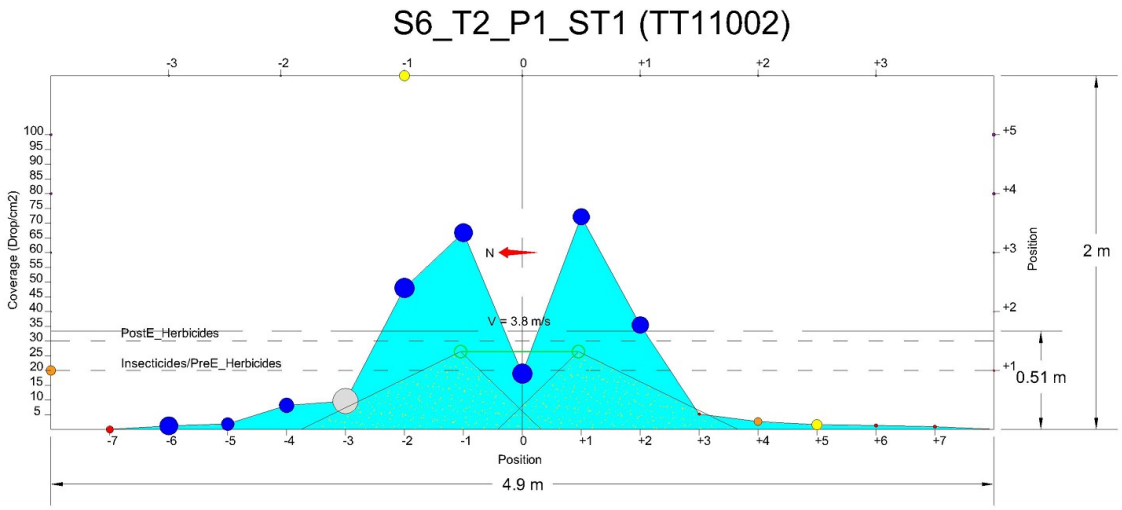

Height (m)	Lat. Position (m)	Velocity (m/s)	Sys. Pressure (Bar)
0.4	-0.01	3.8	2
Temperature (C)	Humidity (RH)	Barometric Pressure (Pa)	
17.02	59.07	98360	

Time	Wind Speed	Wind Direction
-5.23	NA	
-2.62	3.3	E
0.00	3.0	E
2.62	3.3	E
5.23	3.0	E

Figure 3.16: Series 6 - Test 2 - Pass 1 - Station 1

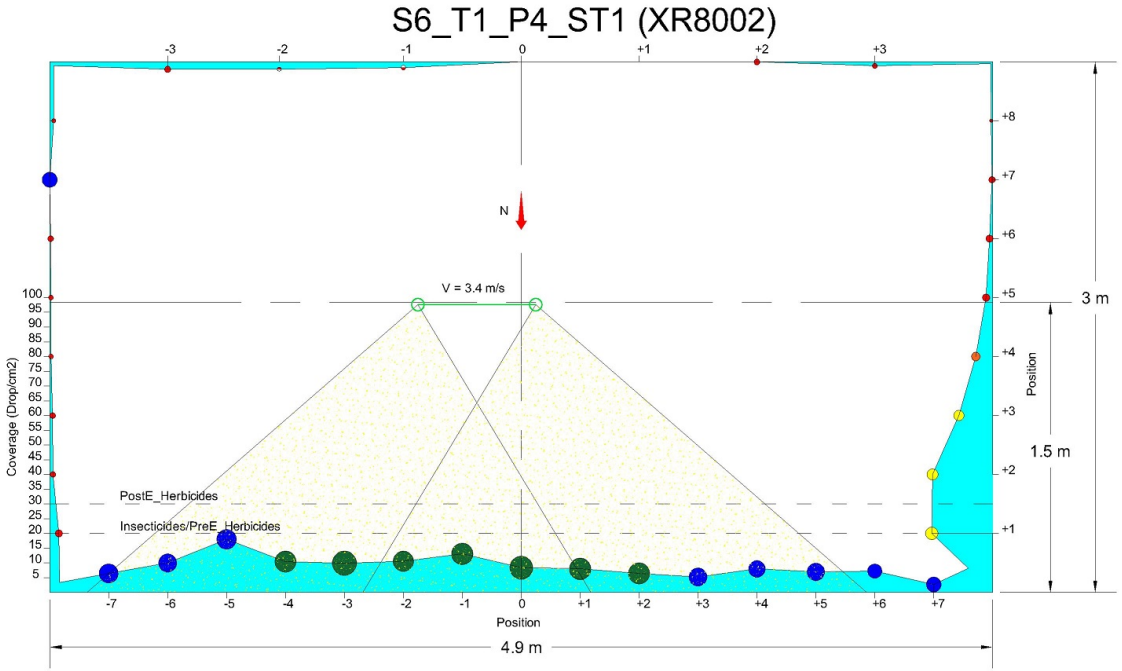

Height (m)	Lat. Position (m)	Velocity (m/s)	Sys. Pressure (Bar)
1.5	-0.23	3.4	2
Temperature (C)	Humidity (RH)	Barometric Pressure (Pa)	
18.32	39.69	99745	

Time	Wind Speed	Wind Direction
NA	NA	NA
-2.62	NA	NA
0.00	2.3	NW
2.62	2.6	NW
5.23	2.0	NW

Figure 3.17: Series 6 - Test 1 - Pass 4 - Station 1

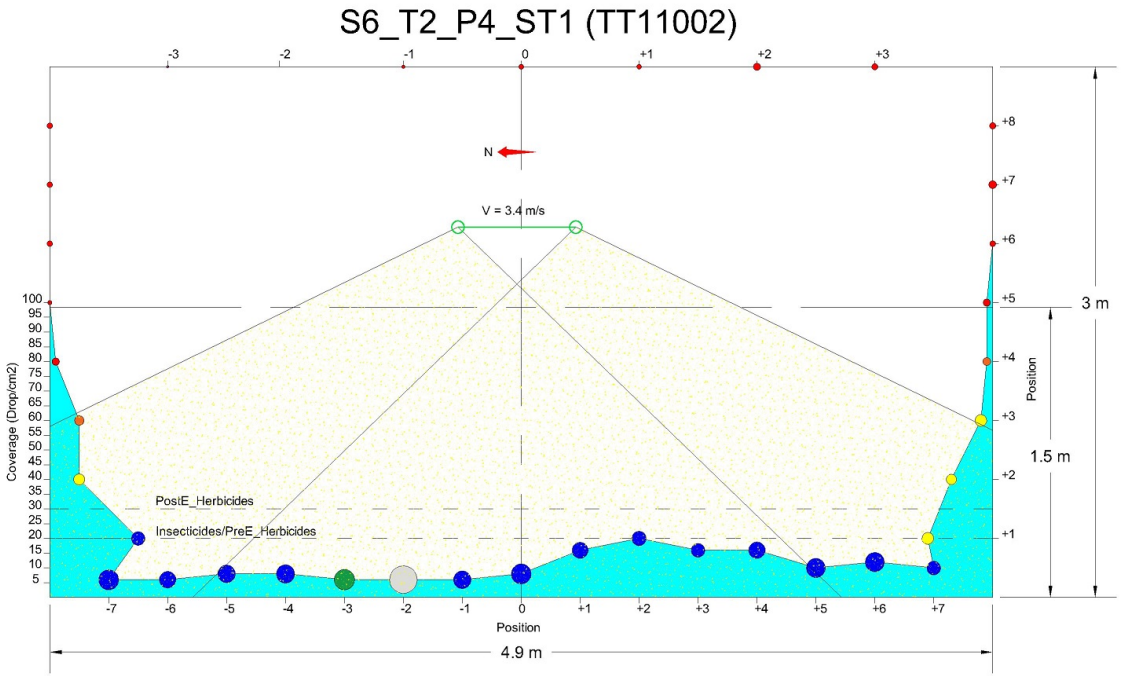

Height (m)	Lat. Position (m)	Velocity (m/s)	Sys. Pressure (Bar)
1.9	-0.02	2.2	2
Temperature (C)	Humidity (RH)	Barometric Pressure (Pa)	
18.48	51.79	98485	

Time	Wind Speed	Wind Direction
-5.23	NA	NA
-2.62	1.0	NW
0.00	0.6	E
2.62	0.6	SE
5.23	0.3	W

Figure 3.18: Series 6 - Test 2 - Pass 4 - Station 1

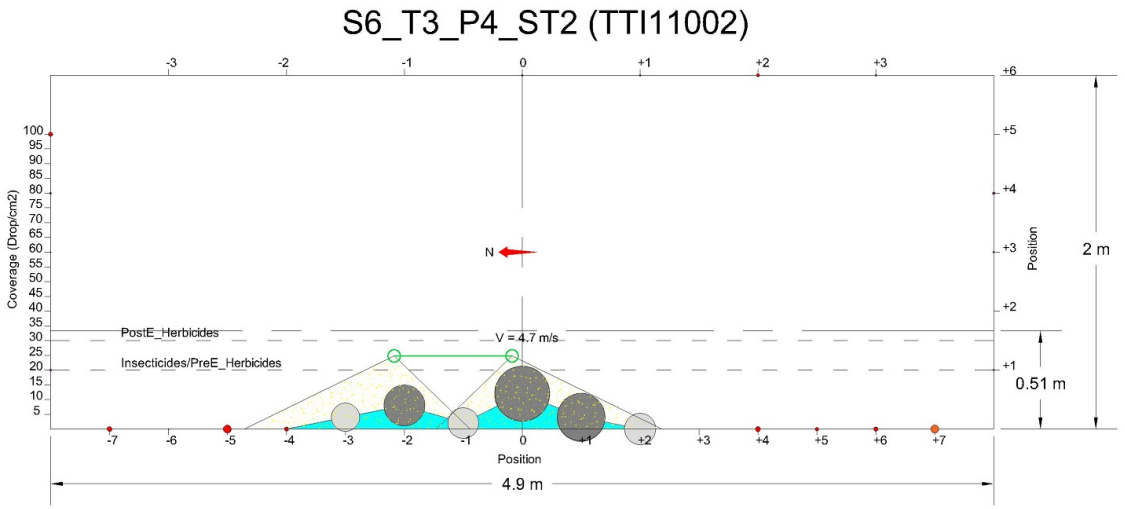

Height (m)	Lat. Position (m)	Velocity (m/s)	Sys. Pressure (Bar)
0.38	-0.36	4.7	2
Temperature (C)	Humidity (RH)	Barometric Pressure (Pa)	
5.54	61.16	99427	

Time	Wind Speed	Wind Direction
-5.22	0.6	NA
-2.61	0.6	NW
0.00	0.6	NW
2.61	0.6	NW
5.22	1.0	NW

Figure 3.19: Series 6 - Test 3 - Pass 4 - Station 2

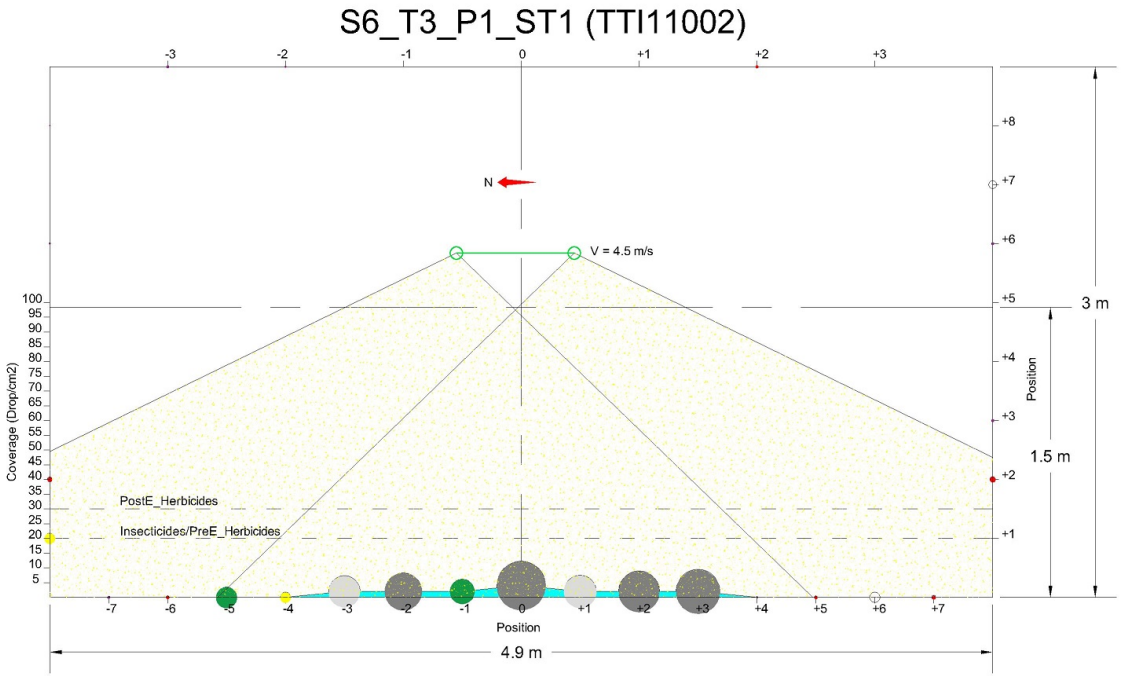

Height (m)	Lat. Position (m)	Velocity (m/s)	Sys. Pressure (Bar)
1.8	-0.03	4.5	2
Temperature (C)	Humidity (RH)	Barometric Pressure (Pa)	
10.12	44.55	99825	

Time	Wind Speed	Wind Direction
NA	NA	NA
-2.61	NA	NA
0.00	0.6	NE
2.63	0.6	NE
5.22	0.6	NE

Figure 3.20: Series 6 - Test 3 - Pass 1 - Station 1

In the case of these tests, CV values were typically quite high (indicating poor uniformity), especially in comparison to larger spray systems, where there are spans of overlapping nozzle spray that generate a band of uniform application between tapered ends. Given the fact that there were only two nozzles and that the nozzles were also at a slight angle directed outward from each other, this uniform band was quite small, resulting in higher average CV values. Comparison to other systems aside, these CV values still indicate application parameters that are best for this type of system, were it to be used for continuous, uniform applications. CV values for all nozzles were higher when application heights were below 1 m (3.3 ft), and slowly decreased above that height (Figure 3.21). This can be observed, for example, between Figures 3.15 and 3.16 where the lower application height is not adequate to allow appropriate overlap of the two nozzles, while the improved uniformity in the latter is countered by the decreased density and loss of smaller droplets due to wind.

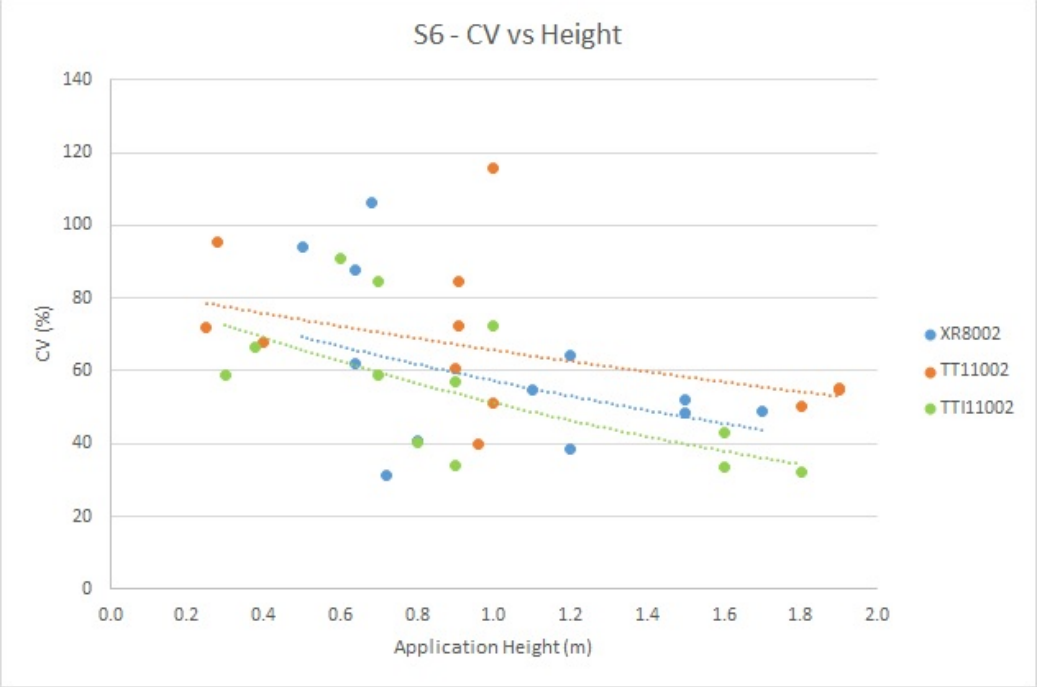

Figure 3.21: Series 6 - Comparison of UAS Height and CV

Despite variation in rotor configuration between a helicopter and a multirotor UAS, these same basic behaviors were observed during testing, and their effects were apparent in several of the XR nozzle results (Figure 3.22). The outflow effects were observed to a lesser degree in the TT nozzle re-

sults and were nearly absent from the TTI results, presumably due to the respective concentrations of droplets below 150 micron as mentioned earlier.

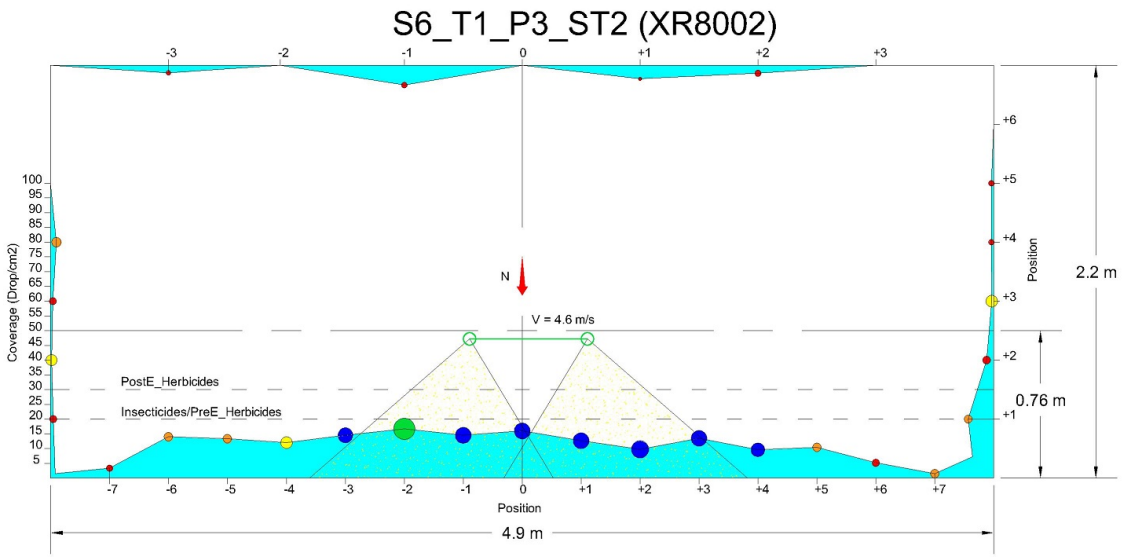

Height (m)	Lat. Position (m)	Velocity (m/s)	Sys. Pressure (Bar)
0.72	0.03	4.6	2
Temperature (C)	Humidity (RH)	Barometric Pressure (Pa)	
15.89	51.41	99656	

Time	Wind Speed	Wind Direction
-5.23	NA	NA
-2.62	1.3	N
0.00	1.3	S
2.62	1.7	NW
5.23	2.3	W

Figure 3.22: Series 6 - Test 1 - Pass 3 - Station 2

Series 2,4 and 6 also demonstrated the high degree of influence both UAS airflow and weather had on smaller droplets, especially with the XR nozzle. In order to better establish the degree to which these factors influenced droplets, the equations listed in [Section] regarding extinction time and terminal velocity, were used to estimate the likelihood droplets of various sizes would evaporate prior to impacting the ground due to gravitational forces. Additionally basic drag calculations could be used via the Equation 3.3:

$$a_D = \frac{\frac{3}{4}\rho C_D}{d} \tag{3.3}$$

Where a_D is the acceleration due to drag (m/s^2), C_D is the drag coefficient (which in this case is assumed to be 1.5, approximately the highest coefficient for a sphere), d is the diameter (m) This also could be used to estimate the influence of wind, and the time it would take for droplets of various size to impact a sample surface perpendicular to the ground, estimating wind as a continuous force based on the average speed taken over the recording time. For simplification, the starting position of each droplet was assumed to be centered at the height of the UAS and have no imparted velocity.

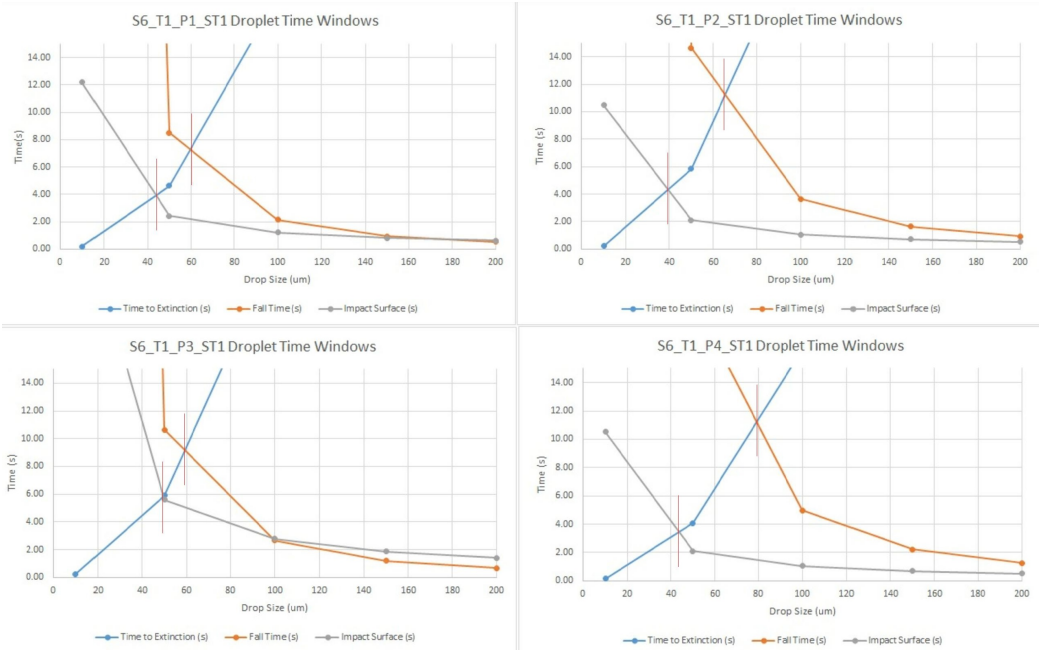

Figure 3.23: Small Droplet Time Windows for XR8002 Nozzle

As previously mentioned, droplets smaller than 150 micron are considered highly susceptible to drift, additionally it can be observed from 3.23 that the

influence of application height, wind speed (as well as downwash) and other meteorological conditions can create significant variability in the lifespan and potential deposit location of droplets below this size, which is observed predominantly in the XR nozzle results and notably in the 8001 nozzle results at high pressures from Series 2 and 4, when the greatest number of small droplets below this size are being produced.

3.2.6 Pattern Capture Estimation

As for Series 2 and 4, an attempt was made to determine the percentage of the spray deposit volume actually captured at each station, relative to an estimate of the spray volume from the nozzles for the short period of time it passed over each station. By evaluating a deposit volume with the respect to the flow rate of the nozzle and UAS velocity, both the actual system deposition efficiency and the sensitivity of the newly developed enclosed test station could be estimated.

The deposit volume density (μL/cm^2) on each water sensitive card was calculated, and then the data from all the cards were used to interpolate the total deposited volume over the total perimeter covered by each station. Data from six stations were compared in an exploratory analysis with the following results, detailing the percentage of the spray deposition volume estimated from the deposit data, compared to the theoretical spray volume calculated based on the system pressure, UAS velocity, and the nozzle flow rate information:

Table 3.4: Series 6 - Pattern Capture Estimates

Test	Nozzle Type	Height (m)	Estimated Percentage
S6-T1-P1-ST1	XR8002	0.64	80%
S6-T1-P1-ST2	XR8002	0.64	112%
S6-T1-P1-ST3	XR8002	0.5	95%
S6-T1-P3-ST1	XR8002	0.8	52%
S6-T1-P4-ST1	XR8002	1.5	74%
S6-T2-P2-ST1	TT11002	1.0	69%

Estimates were also made attempting to compare the theoretical application rate to the averaged spray deposit volume collected in Series 2 and 4. The total recorded deposit volume density was estimated in GPA and compared to theoretical values from the nozzle manufacturer for the recorded speed and pressure. Results displayed in Tables 3.5 and 3.6 show trends matching the previously observed behavior of a deposit volume decrease with a pressure increase for the 8001 nozzle. The lower total estimated percentages relative to the theoretical values can largely be attributed to Series 2 and 4 not including the full pattern width.

Table 3.5: Series 2 - Pattern Capture Estimates

	XR8001	XR8002
Pressure (Bar)	Estimated Percentage	Estimated Percentage
1	73%	56%
3	31%	48%
3	34%	45%
4	23%	45%

Table 3.6: Series 4 - Pattern Capture Estimates

	XR8001	XR8002
Pressure (Bar)	Estimated Percentage	Estimated Percentage
1	65%	70%
3	65%	64%
4	34%	64%

No observable pattern was found within Series 6 based on these results, and the results did not seem to correspond to the characteristics of the flight system or tests. Comparison to results from Series 2 and 4 however, indicate an overall increase in the portion of the pattern volume that was captured by the Series 6 frame. Anomalies within the estimated volume percentages (such as a 112% estimated percentage) highlight deficiencies in the use of linear interpolation with the sample card spacing, which could be improved

by increasing the density of the sample cards in the areas the pattern is most variable.

3.2.7 Ideal Operating Conditions

As mentioned in Section 1.4, the focus of this research was not to determine specific values for pattern characteristics or system conditions, as these would likely only be specific to this system. However observations highlighting these conditions may help provide insight into a starting point for future systems.

For the XR nozzle, representing a nozzle producing a large percentage of droplets below 150 micron, it was found that the ideal flight height to optimize for CV, application density, and pattern width with reduction of off-target percentage was at the manufacturer's suggested application height, with a typical pattern represented in Figure 3.24. The TT nozzle representing a similar nozzle with pattern shifted to a slightly larger droplet size and containing a smaller percentage of droplets under 150 micron, showed a similar behavior, with the application height closest to manufacturer's recommendation, an example demonstrated previously in Figure 3.16. The only nozzle not demonstrating this behavior was the TTI nozzle, which again could be subjected to significant height variations and display little variation in the aforementioned variables.

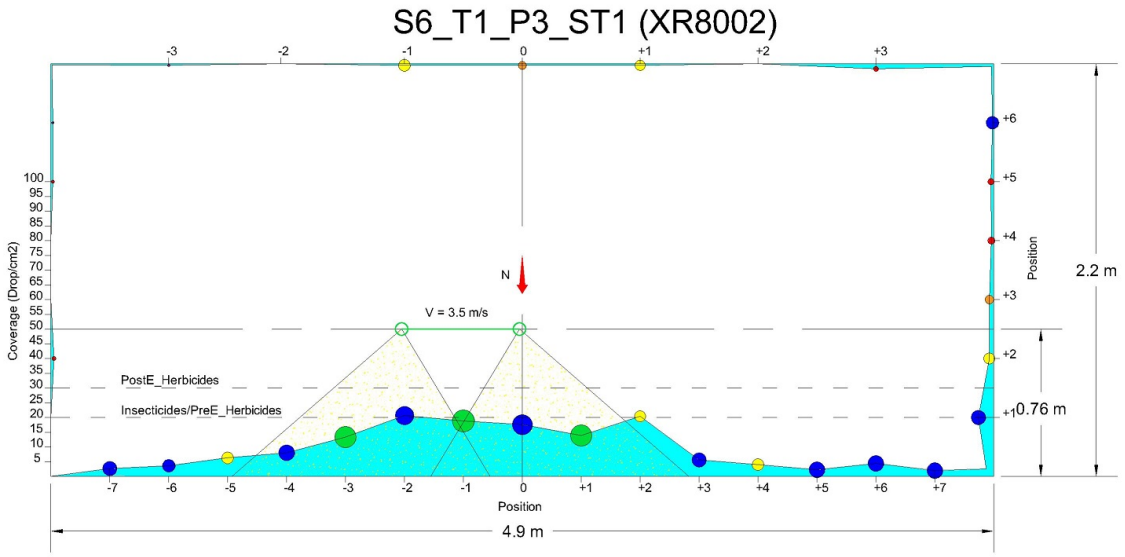

Height (m)	Lat. Position (m)	Velocity (m/s)	Sys. Pressure (Bar)
0.8	-0.32	3.5	2
Temperature (C)	Humidity (RH)	Barometric Pressure (Pa)	
15.8	51.15	99660	

Time	Wind Speed	Wind Direction
NA	NA	NA
-2.62	NA	NA
0.00	1.3	N
2.62	1.3	S
5.23	1.7	NW

Figure 3.24: Series 6 - Test 1 - Pass 3 - Station 1

CHAPTER 4

CONCLUSIONS

The information collected from these experiments provided valuable insight into the behavior of ULV spray patterns applied from multirotor UAS. General observations suggest that the spray pattern does not vary significantly from what manufacturer nozzle tests indicate under optimal application conditions, but notable variations do exist, especially in nozzles producing high quantities of small droplets. Additionally, sensitivity to airflow (from the UAS and meteorological effects) was observed with droplets in the Medium range and smaller, which is also to be expected, but is important to consider when designing a sprayer utilizing this type of platform.

The test system used in Series 6 also allowed a rough estimation of the total deposit volume recovered, compared to the theoretical volume deposited by the nozzles. While this analysis did not yield any clear patterns within Series 6 itself, relative to flight and environmental variables, it demonstrated an overall increase in percentage of the spray pattern captured compared to Series 2 and 4, which represented more typical collection methods used in similar studies. As the estimation of volume relied on interpolation between sample locations, deficiencies were highlighted in the quality of the pattern estimation in areas of high variability (especially directly beneath the UAS when application heights were below manufacturer recommendations). These results highlight the need for an enclosed system equipped with a higher resolution measurement method, in future analysis of this type.

This system demonstrates high sensitivity to off-target application when using nozzles that produce a droplet spectrum containing a significant portion (with respect to volume) of droplets smaller than 150 micron. Off-target application can increase to approximately 50% of the droplet count, at heights above 1m, but were demonstrated to stay under 10% when applied at or below the recommended application height (in this case 0.8 m). While this produced the smallest effective pattern width, and highest CV, the pat-

tern density was significantly higher as well as a significantly lower off-target application percentage. These characteristics highlight the importance of accurate height control if applying with this nozzle type. A system using this nozzle type would require a more robust sensor and control system for height maintenance, but simultaneously could expect much greater droplet density values when applied in weather conditions suitable for spraying [25].

A nozzle producing more droplets in the Medium to Coarse range and a smaller percentage of droplets under 150 micron, such as the TT nozzle, demonstrates similar behavior due to variations in height and speed as the XR nozzle, in regards to effective swath width, and density, but demonstrated lower off-target application numbers. Redistribution of the spray pattern due to meteorological conditions was still observed at higher flight heights, containing the same spectrum of small droplets, but representing a smaller percentage of the spray volume (as is the case with the droplet spectrum produced by this nozzle). The outflow behavior seen in the XR nozzle was also not observed in the TT nozzle to the same degree, likely for the same reason. The implication of these observations being that a nozzle producing droplets in this spectrum, carries much of the benefits described previously, while also further minimizing drift and off-target application potential, when applied at heights at or below the recommended application height.

In addition to a precise flight altitude, a broadcast spray system utilizing either the XR or TT nozzles would likely also require a very precise positioning system. If spray is applied from heights below 0.8 m to minimize drift and off-target application, the effective width of the spray pattern was shown to be between 2 and 3 m. Large spray systems which utilize extensive nozzle arrays mounted on booms, have the advantage of being able to control the overlap of their spray pattern by adjusting nozzle and boom characteristics, positioning is primarily a concern where overlap occurs between passes at the edges of the spray pattern [25]. A small system such as this does not have the advantage of this large span of continuity, and every pass is made up largely of these overlap regions. As a result, poor positioning could have a very drastic effect on the uniformity of overall application. GPS systems, which are currently the most common method of positioning outdoors, generally have accuracies in the scale of meters [29], so given a 2-3 m pattern width, this represents a very large window for error and potential for a relatively non-uniform application. GPS is not likely to be suitable on its own for a

multirotor UAS spray system used as a broadcast applicator, and a more accurate positioning system would be required as well.

Given the low sensitivity to height or meteorological conditions demonstrated in testing, a nozzle producing droplets in the Ultra Coarse and Extremely Coarse range would likely not be subject to the same control limitations. However, as the density was demonstrated to be quite low, a system using this nozzle type would have to travel at a much lower speed, or possibly using a higher flow rate nozzle, depleting its chemical tank much sooner. A system such as this may be more effective for precision application, when the target area is limited to specific areas, and does not require broad application. This type of application has already been demonstrated with ground vehicles and could theoretically be applied to UAS as well [30].

While the test platform used in this experiment varied from those included in Section 1.3, comparison of the results highlights potential deficiencies in the omission of data collection methods, such as those used in Series 6. When sampling only the areas directly beneath the UAS, such as in Series 2-5, much of the information not focused solely on sprayer efficacy in the target area, could be missed, especially when applying from heights significantly higher than those recommended for the nozzles being used (such as in the cited research). The test assembly used in Series 6 could provide a basis for capture of this information in future spray studies.

The phenomena of downwash bias, mentioned in the Roll Balanced UAV study [9] was also observed with the XR nozzle and to a lesser extent the TT nozzle. Larger droplets from these nozzles tended to deposit in the region closer to the UAS center, increasing the VMD in this region, with VMD gradually decreasing in the region of the effective swath and then sharply decreasing outside this area, being attributed to downwash outflow.

One possible side effect of downwash that is worth mentioning is potentially improved coverage on leaf surfaces. Forced airflow through a canopy can result in agitation of crop leaves leading to increased coverage, since the angle of the leaf relative to the spray pattern is continuously varying. Devices such as fans, which generate downward airflow to produce the agitation have even been included on spray systems which do not inherently feature it like aircraft [3]. The effects of the downwash and outflow on penetration through a crop canopy, for a multirotor UAS, warrants further exploration and testing using sampling on leaf surfaces, such as those performed in prior studies [10].

Much of the focus for spray systems has been the increase of coverage area, uniformity, and simplification of application techniques, especially in countries utilizing large, heavy machinery for pesticide application. The development of herbicide resistant crops supported this trend, in making application require less precision, as farmers no longer had to worry about damage to the crops they were spraying. While this resulted in an initial decline in herbicide use, there was an eventual boom in herbicide resistant weed species, requiring continuously increasing doses to eliminate infestations, as farmers became overly dependent on a single herbicide [31]. This resistant behavior is not specific to herbicides, but is probably the most illustrative example. Several options are being proposed as alternatives to this single-pesticide broadcast approach, including systems such as the autonomous patch sprayer [30]. Methods to accurately segment regions of fields using remote sensing, to provide data allowing for site specific treatment of pests, disease, weed infestation, are being developed in order to ensure only regions requiring treatment are targeted, and only the amount needed is applied [32]. This type of precision application would reduce the cost of materials to farmers and the selective pressure for the development of resistance to pesticides [33]. With this type of approach, ability to reach the target area and ease of spray system mobilization to apply in the ideal time windows, could outweigh the importance of how much of the active ingredient an application system can carry and how much can be applied at once. The multirotor UAS design, focused on cheap autonomous operation, could prove an effective platform for this type of application.

Observations made from these tests, and the data sets collected, have provided a tool which can be used to ensure future multirotor UAS applicators can be designed to maximize efficacy, reduce waste, and minimize damage to organisms not being targeted. There are still a wealth of nozzles and application configurations to be tested, but the variety chosen here will ideally provide a broad enough spectrum, that selection of the best parameters for any application can be determined.

REFERENCES

[1] D. Giles and R. Billing, "Deployment and performance of an unmanned aerial vehicle for spraying of specialty crops," in *International Conference of Agricultural Engineering*, Zurich, Germany, jul 2014, pp. 1–7.

[2] "Spraying drone - models," 2017. [Online]. Available: http://sprayingdrone.com/models.html

[3] G. A. Matthews, R. Batemen, and P. Miller, *Pesticide Application Methods*. West Sussex, UK: Wiley Blackwell, 2014.

[4] *The Public Health Impact Of Chemicals: Knowns and Unknowns*, vol. NA, NA 2016.

[5] D. H. Bache and D. R. Johnstone, *Microclimate and Spray Dispersion*. Chichester, UK: Ellis Horwood, 1992.

[6] J. John D. Anderson, *Introduction to Flight*. New York, NY: McGraw-Hill Book Company, 1989.

[7] D. H. Bache and W. J. D. Sayer, "Transport of aerial spray, i. a model of aerial dispersion," *Agricultural Meteorology*, vol. 15, pp. 257–271, oct 1975.

[8] W.-C. Qin, B.-J. Qiu, X.-Y. Xue, C. Chen, Z.-F. Xu, and Q.-Q. Zhou, "Droplet deposition and control effect of insecticides sprayed with an unmanned aerial vehicle against plant hoppers," *Crop Protection*, vol. 85, pp. 79–88, apr 2016.

[9] Y. Bae and Y. M. Koo, "Flight attitudes and spray patterns of a roll-balanced agricultural unmanned helicopter," *Applied Engineering in Agriculture*, vol. 29, pp. 675–682, apr 2013.

[10] W. Qin, X. Xue, L. Zhou, and B. Wang, "Effects of spraying parameters of unmanned aerial vehicle on droplets deposition of maize canopies," *Transactions of the Chinese Society of Agricultural Engineering*, vol. NA, mar 2014.

[11] *Spreading Wings S1000 User Manual*, DJI, nov 2014, v 1.1.

[12] *DX7 Instruction Manual*, Spektrum, nov 2008.

[13] "Arduino uno and genuino uno," 2017. [Online]. Available: https://www.arduino.cc/en/Main/ArduinoBoardUno

[14] *Datasheet SHT1x (SHT10, SHT11, SHT15) Humidity and Temperature Sensor IC*, Sensirion, dec 2011, version 5.

[15] *Xtrinsic MPL3115A2 I2C Precision Altimeter*, Freescale Semiconductor, dec 2013, rev 3.0.

[16] *Weather Sensor Assembly p/n 80422*, Argent Data Systems, NA 2014.

[17] *XBee/XBee-PRO OEM RF Modules*, MaxStream, may 2007, v1.xAx.

[18] *MPU-9150 Product Specification Revision 4.3*, InvenSense, sep 2013, revision 4.3.

[19] *LIDARLite v1 Silver Label Operating Manual*, Pulsed Light, aug 2015.

[20] "Arduino wireless sd shield," 2017. [Online]. Available: https://www.arduino.cc/en/Main/ArduinoWirelessShield

[21] "Arduino zero and genuino zero," 2017. [Online]. Available: https://www.arduino.cc/en/Main/ArduinoBoardZero

[22] *American Sensor Technologies Standard Electrical Connections for AST Pressure Products*, American Sensor Technologies, nov 2013.

[23] "Camera module," 2017. [Online]. Available: https://www.raspberrypi.org/documentation/hardware/camera/

[24] H. Zhu, M. Salyani, and R. D. Fox, "A portable scanning system for evaluation of spray deposit distribution," *Computers and Electronics in Agriculture*, vol. 79, pp. 38–43, jan 2011.

[25] *Catalog 51A-M*, TeeJet, 2014.

[26] "Water-sensitive paper," 2017. [Online]. Available: https://www.syngenta.com.au/awri

[27] D. Nuyttens, K. Baetens, M. D. Schampheleire, and B. Sonck, "Pdpa laser-based characterisation of agricultural spray nozzles," *Agricultural Engineering International: the CIGR Ejournal*, vol. 8, pp. 1–18, dec 2006.

[28] D. E. Johnson, *Applied Multivariate Methods for Data Analysts*. Pacific Grove, CA: Brooks/Cole Publishing, 1998.

[29] "Gps accuracy," 2017. [Online]. Available: http://www.gps.gov/systems/gps/performance/accuracy/

[30] M. G. de Soto, L. Emmi, M. Perez-Ruiz, J. Aguer, and P. G. de Santos, "Autonomous systems for precise spraying - evaluation of a robotised patch sprayer," *Biosystems Engineering*, vol. 146, pp. 165–182, jan 2016.

[31] B. G. Young, "Changes in herbicide use patterns and production practices resulting from glyphosate-resistant crops," *Weed Technology*, vol. 20, pp. 301–307, NA 2006.

[32] R. L. Cointe, T. E. Simon, P. Delarue, M. Herv, M. Leclerc, and S. Poggi, "Reducing the use of pesticides with site-specific application: The chemical control of rhizoctonia solani as a case of study for the management of soil-borne diseases," *PLOS One*, vol. 11, sep 2016.

[33] C. R. Medlina and D. R. Shaw, "Economic comparison of broadcast and site-specific herbicide applications in nontransgenic and glyphosate-tolerant glycine max," *Weed Science*, vol. 48, pp. 653–661, sep 2000.

APPENDIX A: DROPLET DETECTION PROGRAM ALGORITHM

- Import image and establish size
- Detect card boundaries
- Convert to HSV
- Isolate Saturation channel
- Convert to binary edge map using Canny edge detection
- Establish edge locations using Hough line detection
- Detected boundaries are used to establish the size/pixel ratio
- Use detected card bounds to crop image based on input crop value (this value is determined by the user, and is adjusted to remove common sample contamination sources, such as fingerprints on the card edges)
- Droplet isolation
- Image converted to grayscale
- Threshold applied to remove background
- Image converted to binary image
- Enclosed blobs with gaps are filled
- Identify droplets
- Calculate droplet areas
- Convert areas to raw diameters

- Threshold is applied to remove droplets smaller than 2x the size/pixel ratio (to avoid incorrect classification of noise and objects that are too small to accurately be sized) Actual diameters are calculated via Equation 1 [24]:

$$d = 1.06(A0.455) \tag{1}$$

- Droplets are plotted against the original image for visual verification
- Volume, DV1, DV5, DV9, Coverage Density are calculated

APPENDIX B: TEST SERIES DATA PLOTS

The file *SeriesPlots.pdf* contains all data presentation diagrams as described in Section 3.1 for every Series in which the required droplet data was collected to produce the plots (Series 2, Series 4, Series 5, Series 6).

APPENDIX C: WEATHER DATA

The file *SeriesWeather.xls* contains all weather data for Series in which weather was recorded and synced to flights (Series 3, Series 4, Series 5, Series 6).

APPENDIX D: CORRELATION MATRICES

The file *CorrMat.xls* includes all correlation matrices for each test series containing droplet and pattern characterization data (Series 2, Series 4, Series 5, Series 6) with the addition of individual matrices for each Test in Series 6.